



A differential evolution algorithm with a superior-inferior mutation scheme

Meijun Duan¹ · Chun Yu¹ · Shangping Wang² · Bo Li¹

Accepted: 19 June 2023 / Published online: 19 August 2023

© The Author(s), under exclusive licence to Springer-Verlag GmbH Germany, part of Springer Nature 2023

Abstract

A differential evolution (DE) algorithm with superior-inferior mutation scheme (SIDE) is proposed to solve global optimization problems over continuous space. Firstly, a superior-inferior mutation scheme is introduced based on the superior individual and inferior individual. Secondly, the dynamic adjustment strategy of exploration factor for balancing superior individual and inferior individual is proposed, which indicates how much weight to place on local exploitation and global exploration. They are integrated to DE in different milestones of optimization to balance exploration and exploitation of the search space and can alleviate the premature convergence. In order to verify the performance of SIDE, a set of numerical experiments on 32 benchmark functions are executed for performance comparison with 8 advanced DE variants and 4 non-DE-based algorithms for 30, 50 and 100 variables. The experimental results indicate that SIDE is much better than compared DE algorithms in terms of optimization quality. Furthermore, SIDE has the best adaptability to high dimensional problems.

Keywords Differential evolution · Superior-inferior mutation · GLOBAL optimization · Exploration factor

1 Introduction

Differential evolution (DE) is one of the most popular and efficient meta-heuristic optimization algorithms, which is proposed by Storn and Price (1995). It is very popular due to its simplicity and efficient convergence, and it has gained much success in a series of real applications, such as training neural network (Arce et al. 2018), object tracking (Nenavath et al. 2018) and other research and engineering fields. However, slow convergence rate and the

loss of the diversity at the later stage of evolution are the key factors restricting the search performance, which makes DE algorithm get trapped in the local optimum and suffer the premature convergence. In recent years, many variants of DE algorithm have been put forward, which can mainly be categorized into the following 5 types:

- (1) Mutation strategies, which design new mutation strategies to guide the search process (Gong et al. 2013; Tang et al. 2017; Zheng et al. 2017; Cui et al. 2018; Sun et al. 2018; Zhang et al. 2019; Mohamed et al. 2019; Nadimi-Shahraki et al. 2020; Tan and Li 2021; Liu et al. 2021; Yu et al. 2021) or assemble different mutation operators based on the advantages of different mutation modes (Qin et al. 2009; Wang et al. 2011; Mallipeddi et al. 2011; Wu et al. 2016; Wu et al. 2018; Wei et al. 2019; Li et al. 2020a; Zhang et al. 2021a; Hu et al. 2021). Gong et al. (2013) proposed ranking-based mutation operators. Tang et al. (2017) presented a novel decentralizing and coevolving differential evolution (DCDE) algorithm. A novel “DE/current-to-SP-best-ring/1” mutation operation is also proposed in DCDE. Moreover, some researchers combined various

✉ Bo Li
libo@mail.xhu.edu.cn

Meijun Duan
dmj23@163.com

Chun Yu
ycz18@126.com

Shangping Wang
wsp23@163.com

¹ School of Computer and Software Engineering, Xihua University, Chengdu, China

² Science and Technol. On Electronic Information Control Lab., Chengdu, China

mutation strategies based on the advantages of different mutation modes. Zheng et al. (2017) proposed a collective information-powered DE (CIPDE), a collective individual contained in the mutation operator of which is a linear combination of m individuals with optimal fitness values. Cui et al. (2018) put forward an adaptive multiple-elites-guided composite differential evolution algorithm with a shift mechanism (AMECoDEs). Sun et al. (2018) proposed a novel variant of DE with an individual-dependent mechanism that includes an individual-dependent parameter setting and an individual-dependent mutation strategy. Zhang et al. (2019) proposed a multi-layer competitive-cooperative (MLCC) framework to facilitate the competition and cooperation of multiple DEs. Mohamed et al. (2019) proposed the DE variants (EBDE, EBSHADE), in which three different individuals were ranked to participate in mutations, the difference being that the former's individuals were randomly selected from the top p individuals and from the entire population, while the latter three individuals were all randomly chosen from the population. Nadimi-Shahraki et al. (2020) proposed an effective metaheuristic algorithm named multi-trial vector-based differential evolution (MTDE), which combined different search strategies in the form of trial vector producers. Tan and Li (2021) presented a mixed mutation strategy DE algorithm based on deep Q-network (DQN), named DEDQNN, in which a deep reinforcement learning approach realized the adaptive selection of mutation strategy in the evolution process. Liu et al. (2021) proposed a niching differential evolution algorithm (NDE), which incorporated niching methods into differential evolution algorithm. Yu et al. (2021) presented a differential evolution algorithm based on the knee point (named DEAKP), in which the knee solution would guide the search direction of the algorithm. Qin et al. (2009) proposed a self-adaptive DE algorithm (SaDE). Wang et al. (2011) introduced a Composite Differential Evolution algorithm (CoDE). Mallipeddi et al. (2011) employed an ensemble of mutation strategies and control parameters with the DE (EPSDE). Wu et al. (2016) proposed a multi-population ensemble DE (MPEDDE). Wu et al. (2018) focused on the high-level ensemble of different DE variants and proposed a new algorithm named EDEV. Wei et al. (2019) proposed a random perturbation modified differential evolution algorithm (PRMDE), which contained a new “DE/M_pBest-best/1” mutation operator. Li et al. (2020a) proposed an improved differential evolution algorithm with

dual mutation strategies collaboration (DMCDE), in which an elite guidance mechanism and a mechanism of dual mutation strategies collaboration were introduced. Zhang et al. (2021a) put forward a new strategy adaptation method, named explicit adaptation scheme (Ea scheme), which separated multiple strategies and employs them on-demand. Hu et al. (2021) presented a multi-strategy co-evolutionary approach considering a dynamic adaptive selection mechanism and the combination of different characteristic mutation strategies.

- (2) Control parameters adaption or self-adaption strategies, which mainly focus on the adjustment strategies of the amplification factor and crossover probability. Nasimul et al. (2011) proposed a new Adaptive Differential Evolution algorithm (aDE), which adjusts the scaling factor (F) and the crossover probability (CR) adaptively according to the average fitness of parent population and the fitness of offspring individual. Ryoji et al. (2013) proposed a parameter adaptation technique for DE (SHADE) which uses a historical memory of successful control parameters to guide the selection of future control parameters. Gong et al. (2014) proposed a crossover rate repair technique for the adaptive DE algorithms (Rcr-JADE) based on successful parameters. Awad et al. (2016) proposed LSHADE-EpSin to enhance the performance of L-SHADE algorithm. In addition, some scholars have proposed adaptive strategies for the population size (N_p). Awad et al. (2018) et al. proposed ensemble sinusoidal differential evolution with niching-based population reduction (called EsDEr-NR). Li et al. (2020b) proposed an enhanced adaptive differential evolution algorithm (EJADE), which introduced the crossover rate sorting mechanism and a dynamic population reduction strategy.
- (3) Both mutation strategies and control parameters strategies, which design the new mutation strategy and novel control parameters strategies simultaneously to improve the performance of algorithm. Cai et al. (2017) presented a neighborhood-adaptive DE (NaDE). A pool of index-based neighborhood topologies and a neighborhood-dependent directional mutation operator are introduced into NaDE. He et al. (2018) presented a novel DE variant with covariance matrix self-adaptation (DECMSA). Wang et al. (2017) proposed a self-adaptive differential evolution algorithm with improved mutation mode (IMMSADE) by improving “DE/rand/1”. Ali et al. (2017) presented adaptive guided differential evolution algorithm (AGDE). Ali et al. (2018) proposed an enhanced fitness-adaptive differential evolution algorithm with novel mutation (EFADE). Zhang et al.

- (2020) proposed an explicit exploitation and exploration capabilities (EEC) control method named selective-candidate framework with similarity selection rule (SCSS). Xu (2020) presented a novel dual-population adaptive differential evolution (DPADE) algorithm, in which a dual-population framework was employed and an adaptive technology was adopted to adjust two important control parameters and avoid the inappropriate parameters. Tian et al. (2020) proposed a high-performance DE (PDE) algorithm guided by information from individuals with potential. At each generation, the selection probability of each strategy in the strategy pool was determined by the strategy's contribution to the improvement in fitness values. Zhang et al. (2021b) proposed a new multi-objective dynamic differential evolution algorithm with parameter self-adaptive strategies, named SA-MODDE. All components of the algorithm were synergically designed to reach its full potential, containing parental selection, mutation strategy, parameter setting, survival selection, constraint handling, and termination criteria.
- (4) Crossover strategies, which try to expand the search areas to keep the diversity of population. Guo et al. (2015) proposed a crossover operator utilizing eigenvectors of covariance matrix. Xu et al. (2015) proposed the superior-inferior crossover scheme. Cai et al. (2015) proposed hybrid linkage crossover. Ghosh et al. (2017) proposed the optional blending crossover scheme. Qiu et al. (2017) proposed a multiple exponential recombination.
- (5) Hybrid mechanisms, which mainly study the advantages of various evolutionary algorithms and have proposed hybrid algorithms of DE and other EAs. Li et al. (2012) proposed a new hybrid algorithm, called as differential evolution algorithm (DE)/artificial bee colony algorithm (ABC). Vaisakh et al. (2013) came up with a hybrid approach involving Differential Evolution (DE) and BFOA algorithm. Ponsich et al. (2013) hybridized DE with Tabu Search (TS). Le et al. (2013) merged differential evolution and harmony search. Nenavath et al. (2018) proposed a hybrid sine–cosine algorithm with differential evolution algorithm (Hybrid SCA-DE). Myszkowski et al. (2018) presented a hybrid Differential Evolution and Greedy Algorithm (DEGR). Wang et al. (2019) proposed a self-adaptive mutation differential evolution algorithm based on particle swarm optimization (DEPSO). Yildizdan and Baykan (2020) used the bat algorithm (MBA) algorithm in conjunction with the DE algorithm. Nguyen-Van et al. (2021) proposed a novel optimization algorithm as a cross-breed of the DE and the symbiotic organisms

search (SOS). Houssein et al. (2021) proposed a hybrid algorithm: SMA combined to Adaptive Guided Differential Evolution Algorithm (AGDE) (SMA-AGDE). An opposition-based hybrid discrete optimization algorithm that a discrete and Opposition-Based Learning (OBL) version of the Moth-Flame Optimization (MFO) combined with the Differential Evolution (DE) algorithm was proposed by Ahmed et al. (2021). Chakraborty et al. (2021) presented a modified Whale optimization with the success history-based adaptive differential evolution (SHADE-WOA). The differential evolution and sine cosine algorithm based novel hybrid multi-objective evolutionary optimization methods were proposed by Altay and Alatas (2021). Although many kinds of DE variants have been proposed to improve the global optimization performance, they are still unavoidable for getting trapped in the local optima, especially for the complex problems, such as the problem with a very narrow valley from local optimum to global optimum, etc. Finding a proper balance between exploration and exploitation is the most challenging task in the development of any meta-heuristic algorithm due to the stochastic nature of the optimization process. In order to further balance the local exploitation and global exploration ability of DE, a differential evolution with superior-inferior mutation scheme (SIDE) is proposed.

The rest of the paper is structured as follows. Section 2 describes the background materials of DE. Section 3 is devoted to the proposed SIDE algorithm. Section 4 performs numerical experiments and comparisons using 32 benchmark functions of different properties, comparing with 8 DE variants and 4 non-DE-based algorithms. Finally, Sect. 5 presents the conclusions and future work.

2 Background materials of DE

DE is a population-based meta-heuristic global optimization algorithm and a competitive evolutionary algorithm (EA), especially in solving complex numerical optimization problems. Similar to the other evolution algorithms, DE also utilizes mutation, crossover and selection operators. For D-dimensional minimum optimization problems:

$$\begin{cases} \min f(x_1, \dots, x_D) \\ x_j \in [x_j^L, x_j^U], \forall j = 1, \dots, D \end{cases} \quad (1)$$

where x_j^L and x_j^U are respectively the lower bound and upper bound of x_j .

2.1 Mutation

A mutant vector V_i^t for each vector (called target vector here) is obtained by mutation operator based on scaling differences between randomly selected elements of the population to another element. There are many mutation operators available, and the classical one is “DE/rand/2”:

$$V_i^t = X_{r1}^t + F \cdot (X_{r2}^t - X_{r3}^t) + F \cdot (X_{r4}^t - X_{r5}^t) \quad (2)$$

where $F \in [0, 2]$ is the scaling factor, $i = \{1, 2, \dots, N_p\}$, N_p is the population size, t is the generation number, V_i^t is the mutant vector, $r_1, r_2, r_3, r_4, r_5 \in \{1, 2, \dots, N_p\} \setminus \{i\}$ are randomly generated, and $r_1 \neq r_2 \neq r_3 \neq r_4 \neq r_5$.

2.2 Crossover

A trial vector can be constructed by performing crossover operator between a mutant vector and its associated target vector. The diversity of the population can be increased to expand the search area. The most commonly used binomial crossover constructs the trial vector in a random manner, as is described in Eq. (3).

$$U_{i,j}^t = \begin{cases} V_{i,j}^t & \text{if } \text{rand}(0, 1) \leq CR \text{ or } j = j_{rand} \\ X_{i,j}^t & \text{others} \end{cases} \quad (3)$$

where CR is the crossover probability in $[0, 1]$. j_{rand} is randomly chosen from the set $\{1, 2, \dots, D\}$, which guarantees that U_i^t has at least one component from V_i^t .

2.3 Selection

The selection operator determines the survival of the better one between the target vector and the trial vector to the next generation. DE adopts a greedy strategy to determine whether the trial vector or the old target vector survives to the next generation. If and only if the trial vector U_i^t yields a better fitness value than the old target vector X_i^t , then X_i^{t+1} is updated by the trial vector U_i^t . Otherwise, the old target vector X_i^t remains unchanged. The detailed selection scheme is as follows:

$$X_i^{t+1} = \begin{cases} U_i^t & f(U_i^t) < f(X_i^t) \\ X_i^t & \text{others} \end{cases} \quad (4)$$

3 SIDE algorithm

3.1 Superior-Inferior mutation scheme

The population diversity decreases rapidly, which leads to the failure of the clustered individuals to reproduce better individuals. Meanwhile, original DE has the weak local

convergence ability. To further improve the local exploitation capability and global exploration capability of DE, a superior-inferior mutation scheme is proposed.

In superior-inferior mutation scheme, the superior individuals mainly guide the promising searching direction, and the inferior individuals can maintain population diversity in the evolution process. They have different effect to the mutation vector in the different milestones of optimization. The former increases emphasis on local search speeds up convergence without sacrificing the global properties of the algorithm; the latter is used to prevent the algorithm from becoming too local in its orientation, wasting precious function evaluations in pursuit of extremely small improvements.

The proposed superior-inferior mutation scheme is shown in Eq. (5).

$$\begin{aligned} V_i^t = & \omega_{i-1}^t \cdot X_{best}^t + \gamma^t \cdot \omega_{i-2}^t \cdot X_{worst}^t + F \cdot (X_{superior}^t - X_i^t) \\ & + \gamma^t \cdot \omega_{i-2}^t \cdot (X_{inferior}^t - X_i^t) \end{aligned} \quad (5)$$

where t is the generation counter, X_{best}^t and X_{worst}^t are respectively the best individual and worst individual at the current generation. $X_{superior}^t$ and $X_{inferior}^t$ are respectively the superior individual and inferior individual. $X_{superior}^t$, $X_{inferior}^t$ and X_i^t are distinct individuals. The fitness value of $X_{superior}^t$ is better than the parent vector X_i^t , and the fitness value of $X_{inferior}^t$ is worse than the fitness of parent vector X_i^t . ω_{i-1}^t and ω_{i-2}^t serve as a relative weight on local versus global search. if $f(X_i^t) > f_{mean}$, $\omega_{i-1}^t = 1$, $\omega_{i-2}^t = 0$, otherwise, $\omega_{i-1}^t = 0$, $\omega_{i-2}^t = 1$. $f(X_i^t)$ is the fitness value of X_i^t , f_{mean} is the mean fitness value. The larger ω_{i-1}^t is, the higher the relative emphasis puts on local search is. The larger ω_{i-2}^t is, the higher the relative emphasis puts on global search is. γ^t is the exploration factor, which also controls the relative emphasis putting on global search.

As far as the fitness value is concerned, the larger the better. The individuals are sorted in descending order according to the fitness of individuals. After fitness sorting, the top individual is the best, and the bottom individual is the worst. For the i th individual X_i^t , it is the k th individual after sorting in Fig. 1. In our mutation scheme, $X_{superior}^t$ is chosen from the superior set $\{X_1, \dots, X_{k-1}\}$ randomly, and $X_{inferior}^t$ is randomly chosen from the inferior set $\{X_{k+1}, \dots, X_{N_p}\}$.

3.2 Dynamic adjustment strategy of exploration factor γ

Population-based meta-heuristic optimization algorithms share a common feature regardless of their nature. The optimization process can be divided to two phases:

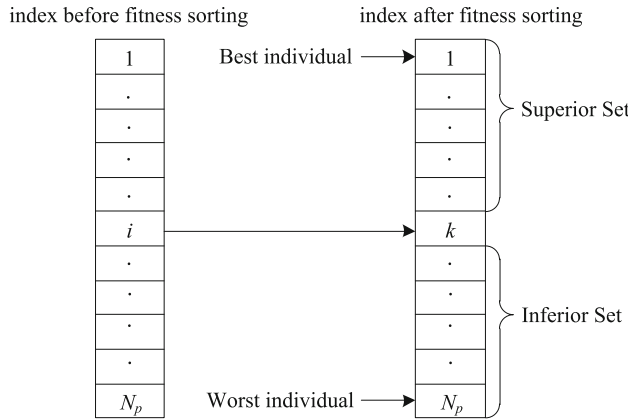


Fig. 1 Superior-inferior mutation scheme

exploration versus exploitation. In the exploration phase, searching the promising regions of the search space with a high rate is important. While, in the exploitation phase,

random variations are considerably less than those in the exploration phase, which leads to lower the population diversity. Based on the above evolutionary property, to make full use of the role of the superior individual and the inferior individual, dynamic adjustment strategies of exploration factor are adopted.

Inferior individual is mainly used to improve the diversity at the later stage of evolution. Therefore, the exploration factor is adjusted dynamically according to sine curve with the generations.

$$\gamma^t = \sin((t/T)^2) \quad (6)$$

The dynamic adjustment curve of exploration factor are shown in the Fig. 2, which take 1000 iterations as an example.

The flow diagram of SIDE is illustrated in Fig. 3.

A detailed description of proposed SIDE algorithm is presented in Algorithm 1.

Algorithm 1

```

#01   Set up the maximum generation  $T = 1000$ , the generation index  $t = 0$ , the amplification factor  $F = 0.1$ , the
      crossover probability  $CR = 0.9$ , create initial population  $X_{i,j}^{(0)}$  randomly,  $\forall i=1, \dots, N_p, j=1, \dots, D$ .
#02   For  $t = 1$  to  $T$  Do
#03     Evaluate  $f(X_i^t) | \forall i = 1, \dots, N_p$ , calculate  $f_{\text{mean}}$ , and find  $X_b^t$ ;
#04     Sort  $f(X_i^t) | \forall i = 1, \dots, N_p$  in descending order;
#05     Update exploration factor  $\gamma^t = \sin((t/T)^2)$ 
#06     For  $i = 1$  to  $N_p$  Do
#07       If  $f(X_i^t) > f_{\text{mean}}^t$ 
#08          $\omega_{i\_1}^t = 1, \omega_{i\_2}^t = 0$ ;
#09       Else
#10          $\omega_{i\_1}^t = 0, \omega_{i\_2}^t = 1$ ;
#11       End If
#12       Create Superior Set  $\{X_1, \dots, X_k\}$  and Inferior Set  $\{X_{k+1}, \dots, X_{N_p}\}$  for each individual  $X_i^t$ ;
#13       Choose the superior individual  $X_{\text{superior}}^t$  and inferior individual  $X_{\text{inferior}}^t$  for each individual  $X_i^t$ ;
#14       For  $j = 1$  to  $D$  Do
#15         Generate  $j_{\text{rand}} = \text{rand}(1, D)$ ;
#16         If  $j = j_{\text{rand}}$  or  $\text{rand}(0, 1) < CR$  Then
#17            $V_i^t = \omega_{i\_1}^t \cdot X_{\text{best}}^t + \gamma^t \cdot \omega_{i\_2}^t \cdot X_{\text{worst}}^t + F \cdot (X_{\text{superior}}^t - X_i^t) + \gamma^t \cdot \omega_{i\_2}^t \cdot (X_{\text{inferior}}^t - X_i^t)$ 
#18         Else
#19            $U_{i,j}^t = X_{i,j}^t$ ;
#20         End If
#21       End For
#22       If  $f(U_i^t) < f(X_i^t)$  Then
#23          $X_i^{t+1} = U_i^t$ ;
#24       Else
#25          $X_i^{t+1} = X_i^t$ ;
#26       End If
#27     End For
#28      $t = t + 1$ 
#29   End While

```

Fig. 2 The adjustment curve of exploration factor

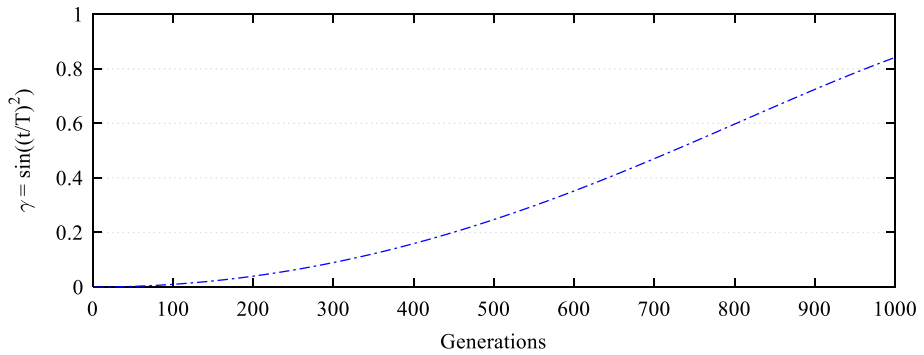
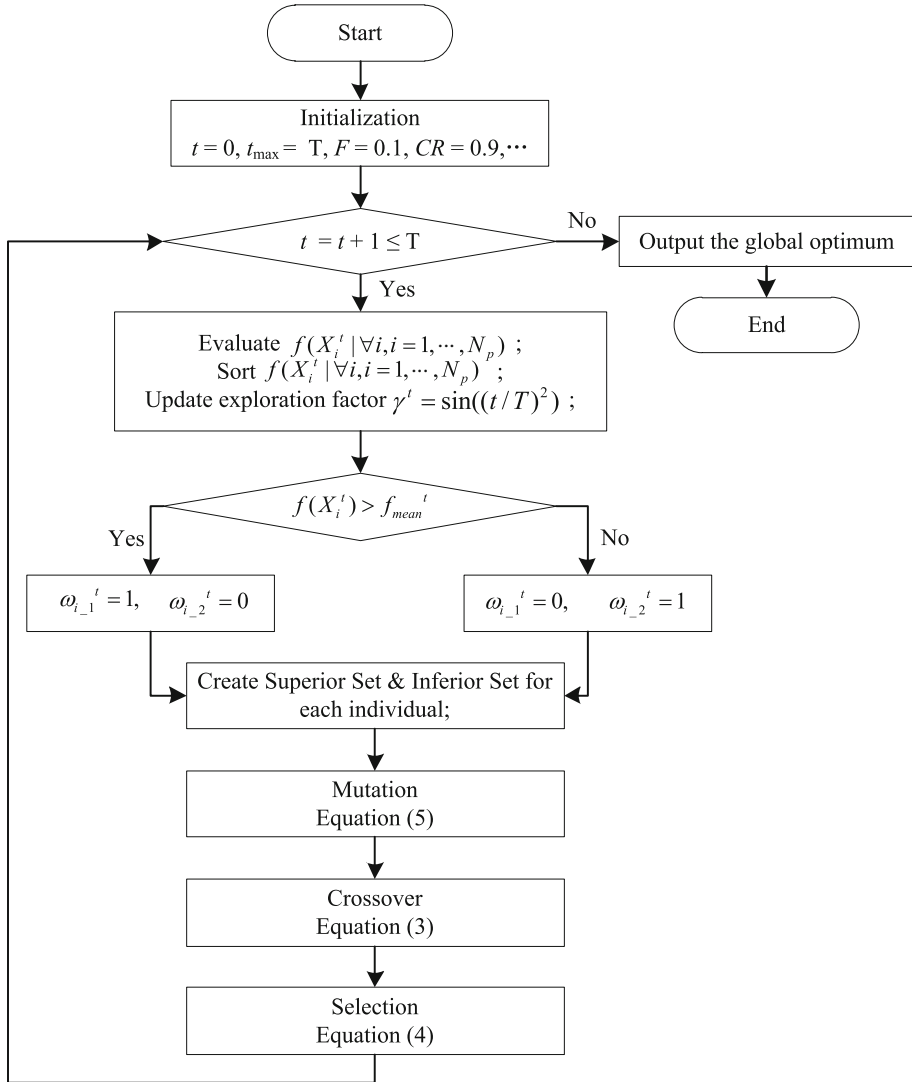


Fig. 3 The flow diagram of SIDE



4 Numerical experiments and comparisons

4.1 Experiments setup

As shown in Table 1, a total of 32 benchmark test functions from literature (Suganthan et al. 2005; Liang et al. 2013;

Awad et al. 2017) are used to perform performance comparison. The properties are as follows: f_1-f_{10} and f_{13} are unimodal functions, f_{11} is step function, f_{12} is noise function, and others are multimodal functions.

4.2 Time complexity

The time complexity is calculated as described in (Suganthan et al. 2005). The codes are implemented in Matlab 2015a and run on a PC with an Intel (R) Core (TM) i5-6500 CPU (3.20 GHz) and 8 GB RAM. The algorithm complexity at $D = 10:10:200$ is plotted in Fig. 4. In Fig. 4, T_0 denotes the running time of the following program:

```
for i = 1 : 1000000
x = (double)5.55;
x = x + x; x = x./2; x = x * x; x = sqrt(x);
x = ln(x); x = exp(x); y = x/x;
end
```

T_1 is the computing time just for Elliptic function for 200,000 evaluations at a certain dimension D . T_2 is the complete computing time for the algorithm with 200,000 evaluations of D dimensional Elliptic Function. T_2 is evaluated five times, and \widehat{T}_2 is used to denote the mean T_2 . At last, the complexity of the algorithm is reflected by: T_0 , T_1 , \widehat{T}_2 , $(\widehat{T}_2 - T_1)/T_0$.

4.3 Comparison with 8 DE variants and 4 non-DE-based algorithms

In order to verify the performance of proposed SIDE, SIDE was compared with 8 advanced DE algorithms which have been reported to have good performance, including MLCCDE (Zhang et al. 2019), EBDE (Mohamed et al. 2019), EDEV (Wu et al. 2018), EsDER-NR (Awad et al. 2018), EJADE (Li et al. 2020b), IMMSADE (Wang et al. 2017), EFADE (Ali et al. 2018), DEPSO (Wang et al. 2019).

- MLCCDE and EBDE are DEs with new mutation strategies.
- EDEV is a composite DE with multiple mutation strategies and control parameters.
- EsDER-NR, EJADE, IMMSADE and EFADE are DEs with an improved mutation strategy and adaptive control parameters.
- DEPSO is a hybrid algorithm of DE and particle swarm optimization (PSO).
- SIDE is also compared with 4 non-DE-based algorithms, including Multi-Verse Optimizer (Mirjalili et al. 2016), Dragonfly algorithm (Mirjalili 2016), Gaining Sharing Knowledge (Ali et al. 2020) and Flow Direction Algorithm (Karami et al. 2021).
- Multi-Verse Optimizer (MVO) is proposed based on three concepts in cosmology: white hole, black hole, and wormhole.

- Dragonfly algorithm (DA): The main inspiration of DA originates from the static and dynamic swarming behaviour of dragonflies in nature.
- Gaining Sharing Knowledge (GSK) mimics the process of gaining and sharing knowledge during the human life span.
- Flow Direction Algorithm (FDA) mimics the flow direction to the outlet point with the lowest height in a drainage basin.

In our experiments, for all the compared algorithms, the associated control parameters are kept the same as the settings in their original papers, which is shown in Table 2. $F = 0.1$ and $CR = 0.9$ are set in SIDE.

To have a reliable and fair comparison, the other common parameters are setting as follows: the population size is set as $N_p = 100$, the maximum generation is set to $T = 1000$ and 30 independent runs are conducted.

4.3.1 Numerical analysis

In this subsection, the numerical results obtained by proposed SIDE are compared with other 12 state-of-the-art algorithms. In the following comparisons, we adopt the solution error ($f(x) - f(x^*)$) to evaluate the optimization performance, where x is the best solution obtained by algorithms in one run, x^* is the global optimum. The Mean and Standard Deviation (STD) of the solution error value are summed up in Tables 3, 4 and 5.

From Tables 3, 4 and 5, SIDE performs better than many compared algorithms and can obtain the global optimal solution on most of test functions, including unimodal functions ($f_1 - f_2$, $f_6 - f_8$, $f_{10} - f_{11}$ and f_{13}) and multi-modal functions ($f_{14} - f_{16}$, $f_{17} - f_{18}$, $f_{13}, f_{24}, f_{26}, f_{28}$ and f_{30}) in all dimensions. Especially, Rastrigin function (f_{14}) has several local minima and it is highly multimodal; Griewank's function (f_{15}) has a component that causes linkage among the dimensions; Ackley function (f_{18}) is characterized by a nearly flat outer region and a large hole at the center; Non-Continuous Rastrigin's Function (f_{28}) is multi-modal, non-separable and asymmetrical function and the local optima's number is huge. For these functions, DE is easy to suffer from premature convergence to be trapped in one of its many local minima. However, SIDE can find the global optimal solution on f_{14}, f_{15}, f_{18} and f_{28} . The reason is that the superior-inferior mutation strategy and the dynamic adjustment strategy of exploration factor assist SIDE in realizing a better balance between local exploitation and global exploration. SIDE can maintain larger diversity to yield better performance. For noise quadric function f_{12} , EJADE, EsDER-NR and MLCCDE are the best at $D = 30$, $D = 50$ and $D = 100$, respectively. Rosenbrock function (f_{19}) have global optimum lays inside

Table 1 Benchmark test functions

Name	Functions	Domain	f_{\min}
Sphere	$f_1(x) = \sum_{i=1}^D x_i^2$	$[-100, 100]^D$	0
Schwefel 1.2	$f_2(x) = \sum_{i=1}^D (\sum_{j=1}^i x_j)^2$	$[-100, 100]^D$	0
Elliptic	$f_3(x) = \sum_{i=1}^D (10^6)^{\frac{i-1}{N-1}} x_i^2$	$[-100, 100]^D$	0
Schwefel 2.22	$f_4(x) = \sum_{i=1}^D x_i + \prod_{i=1}^D x_i $	$[-10, 10]^D$	0
Schwefel 2.21	$f_5(x) = \max\{ x_i , 1 \leq i \leq D\}$	$[-100, 100]^D$	0
SumSquares	$f_6(x) = \sum_{i=1}^D i x_i^2$	$[-10, 10]^D$	0
Exponential	$f_7(x) = -\exp(-0.5 \sum_{i=1}^D x_i^2)$	$[-1, 1]^D$	-1
Tablet	$f_8(x) = 10^6 x_1^2 + \sum_{i=2}^D x_i^2$	$[-100, 100]^D$	0
Zakharov	$f_9(x) = \sum_{i=1}^D x_i^2 + (\sum_{i=1}^D 0.5ix_i)^2 + (\sum_{i=1}^D 0.5ix_i)^4$	$[-5, 10]^D$	0
Bent Cigar	$f_{10}(x) = x_1^2 + 10^6 \sum_{i=2}^D x_i^2$	$[-100, 100]^D$	0
Step	$f_{11}(x) = \sum_{i=1}^D (x_i + 0.5)^2$	$[-100, 100]^D$	0
Noise quartic	$f_{12}(x) = \sum_{i=1}^D ix_i^4 + \text{rand}[0, 1)$	$[-1.28, 1.28]^D$	0
SumPower	$f_{13}(x) = \sum_{i=1}^D x_i ^{(i+1)}$	$[-1, 1]^D$	0
Rastrigin	$f_{14}(x) = \sum_{i=1}^D (x_i^2 - 10 \cos(2\pi x_i) + 10)$	$[-5.12, 5.12]^D$	0
Griewank	$f_{15}(x) = \sum_{i=1}^D x_i^2/4000 - \prod_{i=1}^D \cos(x_i/\sqrt{i}) + 1$	$[-600, 600]^D$	0
Scaffer's F6	$f_{16}(x) = \sum_{i=1}^D (0.5 + \frac{\sin^2(\sqrt{x_i^2+x_{i+1}^2}) - 0.5}{(1+0.001(x_i^2+x_{i+1}^2))^2}) x_{D+1} = x_1$	$[-0.5, 0.5]^D$	0
Salomon	$f_{17}(x) = 1 - \cos(2\pi \sqrt{\sum_{i=1}^D x_i^2}) + 0.1 \sqrt{\sum_{i=1}^D x_i^2}$	$[-100, 100]^D$	0
Ackley	$f_{18}(x) = 20 + e - 20 \exp(-0.2\sqrt{\sum_{i=1}^D x_i^2/D}) - \exp(\sum_{i=1}^D \cos(2\pi x_i)/D)$	$[-32, 32]^D$	0
Rosenbrock	$f_{19} = \sum_{i=1}^{D-1} (100(x_i^2 - x_{i+1})^2 + (x_i - 1)^2)$	$[-100, 100]^D$	0
Scaffer2	$f_{20}(x) = \sum_{i=1}^D (x_i^2 + x_{i+1}^2)^{0.25} (\sin(50(x_i^2 + x_{i+1}^2)^{0.1}) + 1)$	$[-100, 100]^D$	0
Modified Schwefel	$f_{21}(x) = 418.9829 * D - \sum_{i=1}^D g(z_i), z_i = x_i + 4.20968746227503e + 002$ $g(z_i) = \begin{cases} z_i \sin(z_i ^{1/2}) & \text{if } z_i < 500 \\ (500 - \text{mod}(z_i, 500)) \sin(\sqrt{ 500 - \text{mod}(z_i , 500) }) - \frac{(z_i - 500)^2}{1000D} & \text{if } z_i > 500 \\ (\text{mod}(z_i, 500) - 500) \sin(\sqrt{ \text{mod}(z_i , 500) - 500 }) - \frac{(z_i - 500)^2}{1000D} & \text{if } z_i < -500 \end{cases}$	$[-100, 100]^D$	0
HappyCat	$f_{23}(x) = \left (\sum_{i=1}^D x_i^2)^2 - (\sum_{i=1}^D x_i)^2 \right ^{1/2} + (0.5 \sum_{i=1}^D x_i^2 + \sum_{i=1}^D x_i) / D + 0.5$	$[-100, 100]^D$	0
HGBat	$f_{23}(x) = (\sum_{i=1}^D x_i^2)^2 - (\sum_{i=1}^D x_i)^2 ^{1/2} + (0.5 \sum_{i=1}^D x_i^2 + \sum_{i=1}^D x_i) / D + 0.5$	$[-100, 100]^D$	0
Weierstrass	$f_{24}(x) = \sum_{i=1}^D (\sum_{k=0}^{k_{\max}} [a^k \cos(2\pi b^k (x_i + 0.5))]) - D \sum_{k=0}^{k_{\max}} [a^k \cos(2\pi b^k \cdot 0.5)], a = 0.5, b = 3, k_{\max} = 20$	$[-100, 100]^D$	0
Katsuura	$f_{25}(x) = \frac{10}{D^2} \prod_{i=1}^D (1 + i \sum_{j=1}^{32} \frac{ 2^j x_i - \text{round}(2^j x_i) }{2^j})^{\frac{10}{D^2}} - \frac{10}{D^2}$	$[-100, 100]^D$	0
E_ScafferF6	$f_{26}(x) = f_{16}(x_1, x_2) + \dots + f_{16}(x_{D-1}, x_D) + f_{16}(x_D, x_1)$	$[-5, 5]^D$	0

Table 1 (continued)

Name	Functions	Domain	f_{\min}
Griewank + Rosenbrock	$f_{27}(x) = f_{15}(f_{19}(x_1, x_2)) + \dots + f_{15}(f_{19}(x_{D-1}, x_D)) + f_{15}(f_{19}(x_D, x_1))$	$[-3, 1]^D$	0
NCRastrigin	$f_{28} = \sum_{i=1}^D [y_i^2 - 10 \cos(2\pi y_i + 10)], y_i = \begin{cases} x_i, x_i < 0.5 \\ \text{round}(2x_i)/2, x_i \geq 0.5 \end{cases}$	$[-5.12, 5.12]^D$	0
Apline	$f_{29} = \sum_{i=1}^D x_i \sin x_i + 0.1x_i $	$[-10, 10]^D$	0
Bohachevsky_2	$f_{30} = \sum_{i=1}^{D-1} [x_i^2 + 2x_{i+1}^2 - 0.3 \cos(3\pi x_i) \cos(3\pi x_{i+1}) + 0.3]$	$[-100, 100]^D$	0
Levy	$f_{31} = \sin^2(\pi w_1) + \sum_{i=1}^{D-1} (w_i - 1)^2 [1 + 10 \sin^2(\pi w_i + 1)] + (w_D - 1)^2 [1 + \sin^2(2\pi w_D)]$ $w_i = 1 + \frac{x_i - 1}{4}, \forall i = 1, \dots, D$	$[-100, 100]^D$	0
Schwefel's_F7	$f_{32} = \left[\frac{1}{D-1} \sum_{i=1}^{D-1} \left(\sqrt{(x_i^2 + x_{i+1}^2)^{0.5}} \left(\sin \left(50.0 \sqrt{(x_i^2 + x_{i+1}^2)^{0.2}} + 1 \right) \right) \right) \right]^2$	$[-100, 100]^D$	0

a long, narrow, parabolic shaped flat valley, and it is challenging to find the global optimum. For f_{19} , EJADE is the best at $D = 30$ and $D = 50$, and IMMSADE is the best at $D = 100$. Happy Cat function (f_{22}) and HGBat function are multimodal and non-separable functions. For Happy Cat function (f_{22}), MLCCDE is best in all dimensions. Griewank's function has a component that causes linkage among the dimensions and Rosenbrock function is very complex, therefore, expanded Griewank's plus Rosenbrock's function (f_{27}) will be difficult to reach the global optimum. For f_{27} , DEPSO is best in all dimensions. The Schaffer's F7 function (f_{32}) is non-separable, asymmetrical and the local optima's number is huge. For f_{32} , SIDE is the best in all dimensions.

The number of the best and the second best solution error results are listed in Fig. 5. From Fig. 5, SIDE has outstanding performance on most of test functions. SIDE obtains 23 best results out of 32 functions at $D = 30$, while MLCCDE, EBDE, EDEV, EsDER-NR, EJADE, IMMSADE, EFADE, DEPSO, MVO, DA, GSK and FDA obtain 6, 1, 5, 4, 3, 6, 1, 8, 0, 0, 4 and 2 functions, respectively. SIDE keeps this obvious advantage in both 50-D and 100-D problems. However, for other compared algorithms, even for the 30-D dimensions, DEPSO only obtains at most in 8 out of 32 functions.

To further show the performance clearly, we summarize the number of the global optimum graphically in Fig. 6. From the histogram in Fig. 6, for the 30-D dimensions, SIDE obtains 18 global optimums (8 unimodal functions + 10 multi-modal functions), MLCCDE, EBDE, EDEV, EsDER-NR, EJADE, IMMSADE, EFADE, DEPSO, MVO, DA, GSK and FDA only obtain 5 (2 + 3), 0 (0 + 0), 5 (2 + 3), 3 (1 + 2), 1 (1 + 0), 6 (2 + 4), 1 (1 + 0), 7 (2 + 5), 0 (0 + 0), 0 (0 + 0), and 1 (0 + 1) out of 32 functions, respectively. SIDE keeps this obvious advantage in both 50-D and 100-D problems. It is

obviously that the performance superiority of IDE becomes gradually more significant with the increase of the problems' dimension.

In order to illustrate the distribution of the results of each algorithm, the box plots of function solutions of all the algorithms on 6 functions (1 unimodal function and 5 multimodal functions) for the 30-D and 100-D dimensions are depicted in Fig. 7, respectively. It can be seen that SIDE has more concentrated solution error values and fewer outliers compared with other algorithms. Therefore, it can be concluded that SIDE performs more stable than other algorithms on these problems.

Based on the above analysis, it is clear that the proposed SIDE performs well and it has a high exploitation ability and high performance in finding the global solution.

4.3.2 Convergence analysis

The Mean Number of Evolution Generations (MNEG) required to reach the specified convergence precision and the Success Rate (SR) are adopted to analyze the convergence properties. In our experiments, the specified convergence precision is set as 10^{-8} . The MNEG and SR obtained by SIDE, 8 DE variants and 4 non-DE-based algorithms are described in Tables 6, 7 and 8, where “N/A” denotes Not Applicable. For some functions, all the algorithms cannot reach the specified convergence precision, so the MNEG and SR of these functions are omitted in the following tables.

From Tables 6, 7 and 8, we obvious that the MNEG of SIDE is much less than its competitors and the success rate is 100% on $f_1 \sim f_{11}$, $f_{13} \sim f_{18}$, f_{20} , f_{24} , f_{26} and $f_{28} \sim f_{30}$ for all dimensions. It also can be seen that the SIDE has the better performance of convergence rate and outperformed some of other algorithms in terms of stability of solutions. The reasons are as follows: On one hand, the superior

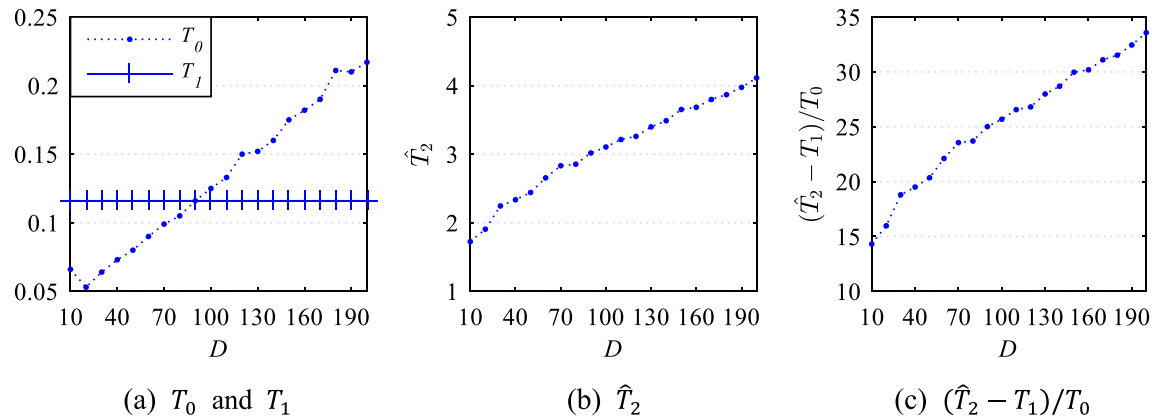


Fig. 4 Time complexity (time in seconds)

Table 2 Parameters setting

Algorithm	Parameters
MLCCDE	$\mu_F = \mu_{CR} = freq = 0.5, G_{LS} = 250, Np_{max} = 18 * D, Np_{min} = 4, H = 5$
EBDE	$p = 0.1, H = 100, M_F(1:H) = M_{CR}(1:H) = 0.5, F = randn(M_F, 0.1), CR = randn(M_{CR}, 0.1)$
EDEV	$\lambda_1 = \lambda_2 = \lambda_3 = 0.1, \lambda_4 = 0.7, ng = 20$
EsDER-NR	$\mu_F = \mu_{CR} = freq = 0.5, G_{LS} = 250, Np_{max} = 18 * D, Np_{min} = 4$
EJADE	$\mu_F = \mu_{CR} = 0.5, c = 0.1, p = 0.05, F = randn(\mu_F, 0.1), CR = randn(\mu_{CR}, 0.1)$
IMMSADE	$\tau = 0.7, \lambda \in [0.7, 1.0], F \in [0.1, 0.8], CR \in [0.3, 1.0]$
EFADE	$\varepsilon = 0.01, CR_1 \in [0.05, 0.15], CR_2 \in [0.9, 1.0]$
DEPSO	$c_1 = c_2 = 2, \omega \in [0.4, 0.9], CR \in [0.3, 1.0], F \in [0.1, 0.8], NS_{max} = 5, \gamma = 0.001, \tau = 0.7, SEP = 0.4 * NP$
MVO	$r_1 \in [0, 1], r_2 \in [0, 1], r_3 \in [0, 1], r_4 \in [0, 1],$
DA	$r_0 = (x^U - x^L)/10, \Delta_{max} = (x^U - x^L)/10$
GSK	$P = 0.1, k_f = 0.5, k_r = 0.9, K = 10$
FDA	$\alpha = 100, \beta = 1$

individuals guide the promising searching direction, so convergence rate will be faster. On the other hand, the dynamic adjustment strategy of exploration factor realizes a better balance of exploration and exploitation, hence SIDE can obtain the better optimization results in most of functions and has the better reliability. Based on the superior-inferior mutation scheme and the dynamic adjustment strategy of exploration factor, the proposed SIDE can better alleviate the premature convergence.

4.3.3 Non-parametric statistical tests

An performance comparison between SIDE and other 12 state-of-the-art algorithms is provided in the above comparisons. To further compare and analyze the solution quality from a statistical angle of different algorithms and to check the behavior of the stochastic algorithms, the results are compared using the following non-parametric statistical tests (Derrac et al. 2011):

- (1) Wilcoxon signed-rank test (to check the differences for each function);
- (2) The Friedman test and Kruskal_Wallis test (to obtain the final rankings of different algorithms for all functions);
- (3) Wilcoxon rank-sum test (to check the differences between SIDE and compared algorithms for all functions).

Wilcoxon's signed-rank test results at the 0.05 significance level for each function are shown in Fig. 8. Signs “+”, “-” and “≈” indicate the number of functions that SIDE is better than, worse than and similar to its competitor, respectively. The Friedman test and Kruskal-Wallis test results are plotted in Fig. 9. Wilcoxon's rank-sum test results are listed in Tables 9, 10 and 11. In Tables 9, 10 and 11, R + denotes the sum of ranks for the test problems in which the first algorithm performs better than the second algorithm, and R - represents the sum of

Table 3 The optimization results obtained by SIDE, 8 DE variants and 4 non-DE-based algorithms at $D = 30$ over independent 30 runs

F	Mean \pm STD	MLCDE	EBDE	EDEV	EsDEt-NR	EJADE	IMMSADE	EFADE	DEPSO	MVO	DA	GSK	FDA	SIDE
f_1	2.66E-31 \pm 3.84E-31	1.31E-44 \pm 2.12E-44	2.34E-31 \pm 1.09E-30	1.80E-54 \pm 1.22E-54	3.72E-44 \pm 1.21E-43	4.41E-28 \pm 1.67E-27	3.64E-12 \pm 5.56E-12	2.27E-99 \pm 1.24E-98	9.75E-02 \pm 2.35E-02	2.96E+02 \pm 4.63E+02	8.55E-28 \pm 3.29E-27	2.39E-19 \pm 3.92E-19	0.00E+00 \pm 0.00E+00	
f_2	4.03E-26 \pm 2.58E-26	1.54E-38 \pm 6.98E-38	1.40E-26 \pm 7.39E-26	3.04E-50 \pm 4.19E-50	2.32E-40 \pm 6.67E-40	8.56E-26 \pm 4.67E-25	4.69E-10 \pm 4.27E-10	1.81E-102 \pm 9.26E-102	3.60E+06 \pm 1.27E+06	6.20E+06 \pm 6.88E+06	1.47E-25 \pm 4.90E-25	1.04E-15 \pm 1.87E-15	0.00E+00 \pm 0.00E+00	
f_3	4.34E-05 \pm 4.59E-05	3.95E-10 \pm 1.52E-09	1.19E-07 \pm 3.35E-07	1.32E-11 \pm 3.14E-11	2.46E-11 \pm 6.95E-11	6.51E+00 \pm 1.63E+01	2.52E+00 \pm 2.63E+00	4.70E-100 \pm 2.52E-99	5.94E+00 \pm 3.07E+00	5.51E+03 \pm 6.01E+03	7.77E-04 \pm 9.71E-04	8.43E-03 \pm 7.09E-03	7.71E-279 \pm 0.00E+00	
f_4	4.51E-14 \pm 4.28E-14	2.70E-23 \pm 6.02E-23	1.18E-14 \pm 4.36E-14	4.60E-26 \pm 2.88E-26	6.13E-19 \pm 1.45E-18	7.96E-17 \pm 3.30E-16	2.80E-05 \pm 6.21E-06	1.94E-51 \pm 1.06E-50	1.99E-01 \pm 4.89E-02	8.14E+00 \pm 5.74E+00	3.56E-16 \pm 1.06E-16	1.43E-12 \pm 1.43E-12	4.94E-324 \pm 0.00E+00	
f_5	1.21E-04 \pm 1.20E-04	4.32E-06 \pm 5.98E-06	1.94E-02 \pm 1.82E-02	5.33E-13 \pm 1.44E-12	1.32E-05 \pm 1.75E-05	2.72E-08 \pm 4.78E-08	2.72E+00 \pm 4.92E-01	1.70E-52 \pm 8.71E-52	3.83E-01 \pm 1.48E-01	9.69E+00 \pm 8.51E+00	1.61E-05 \pm 2.39E-05	1.01E+01 \pm 3.09E+00	5.78E-270 \pm 0.00E+00	
f_6	7.58E-33 \pm 1.21E-32	2.03E-45 \pm 5.19E-45	5.82E-31 \pm 2.72E-30	3.07E-55 \pm 2.46E-55	3.96E-45 \pm 1.67E-44	4.15E-31 \pm 1.46E-30	2.08E-13 \pm 2.06E-13	3.27E-105 \pm 1.79E-104	6.34E-02 \pm 6.33E-02	1.09E+02 \pm 2.16E+02	1.07E-29 \pm 2.80E-29	2.24E-18 \pm 4.24E-18	0.00E+00 \pm 0.00E+00	
f_7	0.00E+00 \pm 0.00E+00	9.25E-17 \pm 4.21E-17	0.00E+00 \pm 0.00E+00	7.40E-18 \pm 2.82E-17	1.37E-16 \pm 4.78E-17	0.00E+00 \pm 0.00E+00	1.25E-10 \pm 4.13E-11	0.00E+00 \pm 0.00E+00	5.20E-06 \pm 1.30E-06	1.69E-02 \pm 2.74E-02	1.00E+00 \pm 5.83E-17	7.03E-16 \pm 7.49E-16	0.00E+00 \pm 0.00E+00	
f_8	1.17E-22 \pm 1.73E-22	1.40E-38 \pm 4.30E-38	3.58E-26 \pm 1.63E-25	2.69E-48 \pm 2.55E-48	5.01E-39 \pm 7.94E-39	9.11E-25 \pm 3.50E-24	3.65E-06 \pm 8.10E-06	2.21E-95 \pm 1.21E-94	8.73E-04 \pm 1.84E+04	3.71E+08 \pm 5.82E+08	6.65E-22 \pm 3.40E-21	8.54E-13 \pm 1.44E-12	0.00E+00 \pm 0.00E+00	
f_9	6.27E-31 \pm 8.53E-31	5.91E-10 \pm 6.75E-10	2.42E-05 \pm 8.19E-05	4.36E-09 \pm 1.12E-08	5.31E-44 \pm 1.39E-43	4.02E+00 \pm 3.42E+00	9.11E-13 \pm 1.11E-12	8.07E-81 \pm 3.50E-80	9.29E-04 \pm 2.24E-04	2.51E+01 \pm 1.81E+01	1.09E+01 \pm 3.19E+00	1.89E-15 \pm 6.83E-15	8.01E-63 \pm 4.38E-62	
f_{10}	9.77E-23 \pm 1.29E-22	2.22E-36 \pm 6.47E-36	1.26E-26 \pm 2.58E-26	5.54E-47 \pm 1.94E-36	4.77E-37 \pm 1.10E-46	1.02E-20 \pm 5.50E-20	1.78E-06 \pm 3.36E-06	5.65E-102 \pm 2.14E-101	9.47E+04 \pm 2.45E+04	1.74E+08 \pm 3.11E+08	4.96E-22 \pm 2.11E-21	2.45E-13 \pm 7.94E-13	0.00E+00 \pm 0.00E+00	
f_{11}	0.00E+00 \pm 0.00E+00	1.33E-01 \pm 3.46E-01	0.00E+00 \pm 0.00E+00	4.50E+00 \pm 3.15E+00	2.65E+02 \pm 3.47E+02	0.00E+00 \pm 0.00E+00	6.33E-01 \pm 9.64E-01							
f_{12}	3.61E-03 \pm 1.12E-03	2.53E-03 \pm 1.09E-03	2.56E-03 \pm 7.91E-04	2.13E-03 \pm 7.04E-04	1.84E-03 \pm 8.99E-04	1.25E+03 \pm 5.75E-06	4.50E-03 \pm 1.77E-03	1.25E+03 \pm 3.43E-06	6.74E-03 \pm 2.60E-03	3.55E-02 \pm 4.29E-02	1.25E+03 \pm 9.79E-06	2.17E-02 \pm 7.69E-03	1.25E+03 \pm 1.36E-05	
f_{13}	7.01E-76	1.97E-78 \pm 1.07E-77	5.12E-69 \pm 2.78E-68	3.62E-116 \pm 1.86E-115	2.70E-101 \pm 1.46E-100	4.77E-96 \pm 2.61E-95	7.46E-63 \pm 2.28E-62	1.66E-126 \pm 9.07E-126	3.67E-08 \pm 2.25E-08	3.82E-06 \pm 8.05E-06	2.17E-48 \pm 7.37E-48	6.78E-39 \pm 2.52E-38	0.00E+00 \pm 0.00E+00	
f_{14}	5.32E+00 \pm 1.59E+00	1.04E-02 \pm 4.29E-02	6.07E-05 \pm 2.45E-04	6.16E-02 \pm 2.25E-01	3.34E+01 \pm 1.82E+01	4.13E+01 \pm 3.25E+01	2.60E+01 \pm 4.49E+00	3.32E-02 \pm 1.82E-01	9.21E+01 \pm 1.81E+01	4.46E+01 \pm 3.71E+01	1.62E+02 \pm 9.37E+01	4.76E+01 \pm 1.79E+01	0.00E+00 \pm 0.00E+00	
f_{15}	0.00E+00 \pm 0.00E+00	3.94E-03 \pm 6.73E-03	0.00E+00 \pm 0.00E+00	3.98E-03 \pm 1.52E-02	2.88E-01 \pm 8.25E-02	0.00E+00 \pm 0.00E+00	2.08E-02 \pm 2.72E-02							
f_{16}	0.00E+00 \pm 0.00E+00	3.70E-18 \pm 2.05E-17	0.00E+00 \pm 0.00E+00	1.07E-16 \pm 5.88E-16	5.05E-06 \pm 1.19E-06	1.73E-02 \pm 3.24E-02	2.96E-15 \pm 3.01E-15	0.00E+00 \pm 0.00E+00						

Table 3 (continued)

<i>F</i>	Mean ± STD	MLCCDE	EBDE	EDEV	ESDer-NR	EJADE	IMMSADE	EFADE	DPSO	MVO	DA	GSK	FDA	SIDE
f_{17}	1.18E-32 ± 1.79E-32	3.06E-45 ± 9.63E-45	6.53E-30 ± 3.55E-29	2.50E-55 ± 2.54E-55	1.26E-45 ± 2.38E-45	1.05E-26 ± 5.73E-26	2.53E-12 ± 2.00E-12	7.75E-107 ± 4.21E-106	2.89E-02 ± 7.36E-03	3.24E+01 ± 4.89E+01	6.58E-30 ± 2.36E-29	5.62E-20 ± 9.36E-20	0.00E+00 ± 0.00E+00	
f_{18}	6.51E-15 ± 1.64E-15	3.10E-02 ± 1.70E-01	3.79E-15 ± 9.01E-16	3.67E-15 ± 6.49E-16	1.61E-14 ± 5.00E-15	3.79E-15 ± 1.30E-15	8.46E-05 ± 2.09E-05	0.00E+00 ± 0.00E+00	3.40E-01 ± 4.93E-01	4.77E+00 ± 3.29E+00	2.38E-14 ± 1.16E-14	2.44E+00 ± 4.37E-01	0.00E+00 ± 0.00E+00	
f_{19}	1.34E-01 ± 7.81E-01	2.20E+00 ± 1.95E+00	5.71E+00 ± 1.58E+00	1.11E+01 ± 1.95E+00	6.65E-01 ± 1.51E+00	2.59E+01 ± 1.53E-01	3.17E+01 ± 2.10E+01	2.78E+01 ± 4.14E-01	1.35E+03 ± 2.59E+03	1.26E+07 ± 6.56E+07	1.36E+01 ± 2.38E+00	2.53E+01 ± 2.50E+01	2.89E+01 ± 4.32E-02	
f_{20}	5.94E-02 ± 2.08E-02	1.32E+00 ± 1.01E+00	1.71E-01 ± 8.76E-02	9.30E-02 ± 1.66E-01	4.05E+00 ± 1.52E+00	2.42E-05 ± 5.63E-05	4.52E+00 ± 3.29E-01	3.27E-26 ± 1.51E-25	1.03E+02 ± 3.70E+01	4.47E+01 ± 2.72E+01	5.96E-02 ± 5.50E-02	8.25E+01 ± 1.89E+01	0.00E+00 ± 0.00E+00	
f_{21}	3.82E-04 ± 0.00E+00	3.82E-04 ± 4.61E-13	3.82E-04 ± 0.00E+00	3.82E-04 ± 0.00E+00	3.82E-04 ± 1.14E-12	3.82E-04 ± 0.00E+00	3.82E-04 ± 0.00E+00	3.82E-04 ± 2.88E-09	3.82E-04 ± 0.00E+00	7.38E+01 ± 1.79E+02	1.38E+02 ± 1.85E+02	3.82E-04 ± 1.07E-12	3.82E-04 ± 0.00E+00	
f_{22}	2.45E-01 ± 3.73E-02	2.30E-01 ± 4.56E-02	2.07E-01 ± 3.78E-02	2.36E-01 ± 3.32E-02	2.74E-01 ± 5.65E-02	4.34E-01 ± 6.80E-02	4.74E-01 ± 6.65E-02	8.35E-01 ± 1.02E-01	7.46E-01 ± 1.57E-01	6.86E+00 ± 7.01E+00	2.90E+01 ± 4.64E-02	5.03E-01 ± 1.31E-01	9.36E-01 ± 1.84E-01	
f_{23}	3.08E-01 ± 9.43E-02	4.69E-01 ± 1.93E-01	3.59E-01 ± 1.08E-01	3.73E-01 ± 1.36E-01	3.74E-01 ± 9.80E-02	0.00E+00 ± 1.01E-01	3.97E-01 ± 3.27E-02	3.32E-01 ± 2.92E-02	4.99E-01 ± 2.68E-03	7.97E-01 ± 4.65E-01	1.63E+02 ± 2.49E+02	4.16E-01 ± 4.64E-02	5.99E-01 ± 9.74E-02	
f_{24}	1.02E-11 ± 5.80E-12	2.58E-02 ± 2.22E-02	1.01E-07 ± 4.34E-07	1.39E-03 ± 5.45E-03	9.07E-02 ± 1.01E-01	0.00E+00 ± 1.01E-01	0.00E+00 ± 7.52E-04	0.00E+00 ± 7.52E-04	7.66E+00 ± 3.28E+00	7.48E+00 ± 4.79E+00	2.51E-04 ± 4.05E-04	1.40E+00 ± 9.34E-01	0.00E+00 ± 0.00E+00	
f_{25}	2.25E-02 ± 2.44E-03	3.21E-03 ± 6.56E-04	1.00E-02 ± 1.74E-03	5.01E-03 ± 1.21E-03	9.16E-02 ± 3.97E-02	6.01E-01 ± 7.87E-02	1.14E-01 ± 1.50E-02	5.31E-01 ± 6.88E-02	9.80E-02 ± 5.07E-02	4.19E-03 ± 5.18E-03	2.25E+00 ± 3.07E-01	0.00E+00 ± 0.00E+00	1.86E-03 ± 3.79E-03	
f_{26}	4.31E-01 ± 6.40E-02	5.42E-01 ± 6.63E-02	1.22E+00 ± 1.98E-01	4.85E-01 ± 6.53E-02	5.62E-01 ± 8.79E-02	8.70E+00 ± 4.92E-01	4.80E+00 ± 3.90E-01	4.51E+00 ± 5.52E-01	1.89E+00 ± 8.01E-01	1.89E+00 ± 1.30E+00	6.91E+00 ± 5.27E-01	1.20E+00 ± 5.06E-01	0.00E+00 ± 0.00E+00	
f_{27}	2.37E-00 ± 3.43E-01	2.18E+00 ± 1.63E-01	3.54E+00 ± 5.65E-01	2.08E+00 ± 1.82E-01	3.39E+00 ± 5.26E-01	1.19E+01 ± 1.08E+00	6.71E+00 ± 7.33E-01	0.00E+00 ± 0.00E+00	5.98E+00 ± 2.01E+00	2.03E+01 ± 7.01E+00	1.62E+01 ± 8.24E-01	1.32E+01 ± 4.31E+00	1.28E+01 ± 3.75E-01	
f_{28}	9.87E+00 ± 1.62E+00	2.90E-03 ± 2.48E-03	5.95E-01 ± 5.12E-01	6.31E-01 ± 5.86E-01	3.68E+01 ± 1.35E+01	5.20E+01 ± 7.55E+00	2.11E+01 ± 1.13E+00	4.77E+01 ± 4.30E+01	1.54E+02 ± 3.85E+01	4.30E+01 ± 2.56E+01	1.33E+02 ± 1.15E+01	3.44E+01 ± 1.23E+01	0.00E+00 ± 0.00E+00	
f_{29}	1.54E-03 ± 5.41E-04	1.82E-19 ± 4.91E-19	1.55E-03 ± 5.04E-04	6.29E-07 ± 3.44E-06	8.54E-17 ± 2.10E-16	4.20E-15 ± 1.23E-14	9.22E-03 ± 8.62E-04	1.09E-55 ± 5.42E-55	3.14E+00 ± 1.82E+00	3.46E+00 ± 4.33E+00	4.03E-09 ± 4.33E+00	9.38E-12 ± 2.01E-08	1.22E-12 ± 2.46E-11	
f_{30}	0.00E+00 ± 0.00E+00	1.10E+00 ± 1.07E+00	0.00E+00 ± 0.00E+00	1.38E-02 ± 7.54E-02	3.07E-02 ± 1.17E-01	0.00E+00 ± 0.00E+00	1.41E-08 ± 1.73E-08	0.00E+00 ± 0.00E+00	6.75E+00 ± 1.32E+00	5.44E+02 ± 8.35E+02	3.70E-18 ± 2.03E-17	8.37E-01 ± 1.11E+00	0.00E+00 ± 0.00E+00	
f_{31}	1.48E-26 ± 2.62E-26	3.58E-01 ± 5.67E-01	2.38E-26 ± 5.92E-26	5.12E-02 ± 1.23E-01	9.64E-02 ± 1.76E-01	1.56E-02 ± 4.90E-03	2.87E-09 ± 5.46E-09	2.15E+00 ± 1.60E-01	2.69E+01 ± 1.84E+01	3.28E+03 ± 5.37E+03	5.45E-28 ± 1.37E-27	1.95E+04 ± 2.70E+03	2.76E+00 ± 2.63E-01	
f_{32}	5.45E-03 ± 3.28E-03	8.43E-03 ± 3.34E-03	5.68E-02 ± 2.26E-02	4.47E-03 ± 1.65E-03	5.93E-01 ± 5.01E-01	9.78E-01 ± 4.12E-01	2.30E-01 ± 7.10E-02	1.80E-05 ± 2.80E-05	2.55E-02 ± 4.10E-02	8.44E-01 ± 1.88E+00	4.72E+00 ± 9.45E-01	3.61E-02 ± 5.63E-02	1.38E-07 ± 6.46E-07	

The best results are highlighted in bold

Table 4 The optimization results obtained by SIDE, 8 DE variants and 4 non-DE-based algorithms at $D = 50$ over independent 30 runs

F	Mean \pm STD	MLCDE	EBDE	EDEV	EsDEr-NR	EJADE	IMMSADE	EFADE	DEPSO	MVO	DA	GSK	FDA	SIDE
f_1	4.72E-18 \pm 4.08E-18	3.03E-23 \pm 7.15E-23	9.50E-23 \pm 2.39E-22	1.91E-32 \pm 6.57E-32	1.59E-24 \pm 3.67E-24	2.02E-21 \pm 1.07E-20	1.95E-04 \pm 1.31E-04	6.63E-101 \pm 1.83E-100	7.97E-01 \pm 1.19E-01	2.76E+02 \pm 2.56E+02	2.59E-14 \pm 2.49E-14	3.70E-09 \pm 4.26E-09	0.00E+00 \pm 0.00E+00	
f_2	3.22E-14 \pm 2.97E-14	8.98E-18 \pm 2.89E-17	5.34E-19 \pm 1.42E-18	1.10E-22 \pm 4.71E-22	9.89E-20 \pm 1.65E-19	3.27E-16 \pm 1.25E-15	2.24E-02 \pm 1.44E-02	9.03E-96 \pm 4.39E-95	3.51E+06 \pm 1.43E+06	1.77E+07 \pm 2.57E+07	1.22E-08 \pm 5.14E-08	2.46E-05 \pm 3.35E-05	0.00E+00 \pm 0.00E+00	
f_3	8.11E+00 \pm 5.80E+00	2.60E-02 \pm 2.83E-02	2.07E-01 \pm 2.40E-01	3.02E-01 \pm 3.40E-01	9.92E-03 \pm 1.01E-02	6.06E+02 \pm 7.78E+02	7.37E+02 \pm 2.53E+02	6.02E-84 \pm 3.30E-83	2.18E+02 \pm 5.26E+01	1.01E+04 \pm 1.40E+04	2.12E+01 \pm 1.18E+01	9.98E+00 \pm 5.76E+00	2.23E-225 \pm 0.00E+00	
f_4	1.06E-09 \pm 4.41E-10	9.27E-11 \pm 4.24E-10	1.97E-11 \pm 5.34E-11	1.64E-10 \pm 3.74E-10	1.46E-09 \pm 2.55E-09	3.63E-13 \pm 1.08E-12	2.12E-02 \pm 4.49E-03	3.07E-50 \pm 1.44E-49	8.17E-01 \pm 1.76E-01	1.04E+01 \pm 7.23E+00	6.83E-08 \pm 2.47E-07	5.51E-07 \pm 2.85E-07	4.94E-324 \pm 0.00E+00	
f_5	3.22E-01 \pm 1.51E-01	1.43E+00 \pm 6.77E-01	2.87E+00 \pm 1.05E+00	4.11E-02 \pm 3.13E-02	7.98E-01 \pm 3.70E-01	1.67E-05 \pm 5.40E-05	1.95E+01 \pm 1.76E+00	1.85E-49 \pm 7.01E-49	1.67E+00 \pm 4.21E-01	1.13E+01 \pm 9.99E+00	2.59E-01 \pm 1.35E-01	1.55E+01 \pm 2.85E+00	3.60E-264 \pm 0.00E+00	
f_6	8.91E-19 \pm 5.54E-19	7.11E-24 \pm 1.06E-23	1.14E-23 \pm 1.88E-23	1.32E-33 \pm 3.55E-33	2.71E-25 \pm 6.82E-25	3.01E-22 \pm 1.65E-21	3.72E-05 \pm 3.31E-05	1.93E-99 \pm 8.25E-99	9.93E-01 \pm 6.94E-01	1.55E+02 \pm 2.12E+02	1.29E-14 \pm 1.78E-14	1.23E-09 \pm 1.84E-09	0.00E+00 \pm 0.00E+00	
f_7	1.04E-16 \pm 2.83E-17	1.78E-16 \pm 5.53E-17	0.00E+00 \pm 0.00E+00	1.52E-16 \pm 5.44E-17	4.33E-16 \pm 1.18E-16	0.00E+00 \pm 0.00E+00	4.02E-06 \pm 1.06E-06	0.00E+00 \pm 0.00E+00	3.68E-05 \pm 9.22E-06	3.11E-02 \pm 4.02E-02	1.00E+00 \pm 5.28E-16	3.24E-09 \pm 3.46E-09	0.00E+00 \pm 0.00E+00	
f_8	4.01E-12 \pm 3.13E-12	3.34E-17 \pm 7.45E-17	1.51E-17 \pm 2.30E-17	3.87E-27 \pm 8.65E-27	1.46E-18 \pm 2.41E-18	1.47E-16 \pm 5.93E-16	2.28E+02 \pm 1.43E+02	9.08E-93 \pm 3.46E-92	7.83E+05 \pm 1.09E+05	9.18E+08 \pm 9.21E+08	1.28E-07 \pm 2.74E-07	4.77E-03 \pm 5.75E-03	0.00E+00 \pm 0.00E+00	
f_9	1.69E-17 \pm 1.22E-17	2.49E-04 \pm 2.05E-04	1.35E-02 \pm 4.96E-02	4.26E-01 \pm 1.16E+00	2.17E-24 \pm 2.88E-24	2.06E+01 \pm 1.18E+01	8.05E-06 \pm 6.41E-06	5.23E-63 \pm 2.87E-62	1.87E+07 \pm 1.94E+07	2.02E+02 \pm 1.40E+02	7.55E+01 \pm 1.61E+01	5.05E-08 \pm 1.26E-07	1.17E-37 \pm 6.21E-37	
f_{10}	4.75E-12 \pm 4.07E-12	3.57E-16 \pm 7.19E-16	5.22E-17 \pm 1.77E-16	2.36E-21 \pm 6.30E-21	1.87E-17 \pm 4.17E-17	1.97E-15 \pm 7.44E-15	1.84E+02 \pm 1.53E+02	2.66E-94 \pm 1.18E-93	6.95E+05 \pm 1.15E+05	5.05E+08 \pm 6.15E+08	2.91E-06 \pm 1.22E-05	3.58E-03 \pm 3.91E-03	0.00E+00 \pm 0.00E+00	
f_{11}	0.00E+00 \pm 0.00E+00	5.23E+00 \pm 3.64E+00	0.00E+00 \pm 0.00E+00	1.00E+00 \pm 9.47E-01	8.33E-01 \pm 1.15E+00	0.00E+00 \pm 0.00E+00	0.00E+00 \pm 0.00E+00	0.00E+00 \pm 0.00E+00	1.82E+01 \pm 8.02E+00	1.37E+03 \pm 1.56E+03	0.00E+00 \pm 0.00E+00	5.13E+00 \pm 2.67E+00	0.00E+00 \pm 0.00E+00	
f_{12}	7.09E-03 \pm 1.78E-03	1.19E-02 \pm 4.71E-03	7.36E-03 \pm 2.90E-03	6.42E-03 \pm 2.41E-03	8.74E-03 \pm 3.92E-03	3.42E+03 \pm 5.00E-06	1.00E-02 \pm 2.90E-03	3.42E+03 \pm 5.33E-06	9.91E-02 \pm 2.92E-02	1.77E-01 \pm 1.58E-01	3.42E+03 \pm 7.81E-01	8.19E-02 \pm 1.89E-02	3.42E+03 \pm 9.47E-06	
f_{13}	6.32E-57	3.14E-50 \pm 1.40E-49	2.99E-50 \pm 9.86E-50	3.46E-69 \pm 1.89E-68	4.82E-69 \pm 1.69E-68	3.34E-77 \pm 1.83E-76	1.64E-52 \pm 6.95E-52	2.20E-122 \pm 1.06E-121	5.10E-11 \pm 6.14E-11	4.03E-07 \pm 5.58E-07	1.03E-32 \pm 5.53E-32	2.13E-26 \pm 5.86E-26	0.00E+00 \pm 0.00E+00	
f_{14}	2.76E+01 \pm 4.13E+00	3.66E+00 \pm 4.12E+00	2.05E+01 \pm 2.94E+00	6.62E+00 \pm 1.58E+00	6.84E+01 \pm 5.34E+01	1.31E+02 \pm 8.67E+01	1.33E+02 \pm 7.64E+00	1.37E-01 \pm 5.89E-01	1.25E+02 \pm 2.51E+01	9.89E+01 \pm 9.21E+01	3.29E+02 \pm 1.74E+01	7.62E+01 \pm 1.81E+01	0.00E+00 \pm 0.00E+00	
f_{15}	3.70E-18 \pm 2.03E-17	1.31E-02 \pm 1.59E-02	3.29E-04 \pm 1.80E-03	2.71E-03 \pm 4.31E-03	2.79E-03 \pm 5.74E-03	0.00E+00 \pm 0.00E+00	2.15E-02 \pm 1.16E-02	0.00E+00 \pm 0.00E+00	6.67E-01 \pm 7.41E-02	1.05E+01 \pm 1.23E+01	2.79E-13 \pm 8.20E-13	3.00E-02 \pm 3.67E-02	0.00E+00 \pm 0.00E+00	
f_{16}	0.00E+00 \pm 0.00E+00	4.81E-17 \pm 6.95E-17	0.00E+00 \pm 0.00E+00	1.11E-17 \pm 4.47E-17	3.00E-16 \pm 2.14E-16	0.00E+00 \pm 0.00E+00	1.12E-08 \pm 9.42E-09	0.00E+00 \pm 0.00E+00	3.78E-05 \pm 5.90E-06	6.87E-02 \pm 7.57E-02	5.55E-17 \pm 1.16E-16	2.43E-08 \pm 5.13E-08	0.00E+00 \pm 0.00E+00	

Table 4 (continued)

<i>F</i>	Mean ± STD	MLCODE	EBDE	EDEV	EsDef-NR	EJADE	IMMSADE	EFADE	DEPSO	MVO	DA	GSK	FDA	SIDE
f_{17}	5.25E-19 ± 3.57E-19	3.19E-24 ± 8.91E-24	7.82E-24 ± 1.57E-23	3.75E-35 ± 6.24E-35	9.72E-26 ± 2.21E-25	1.23E-23 ± 6.71E-23	1.60E-04 ± 1.05E-04	1.81E-98 ± 9.81E-98	2.03E-01 ± 3.98E-02	1.35E+02 ± 2.98E+02	5.54E-14 ± 1.03E-13	2.14E-09 ± 2.93E-09	0.00E+00 ± 0.00E+00	
f_{18}	4.18E-10 ± 2.18E-10	1.69E+00 ± 6.19E-01	2.38E-12 ± 3.12E-12	1.22E-01 ± 3.18E-01	3.88E-13 ± 6.30E-13	4.49E-13 ± 1.86E-12	3.30E-02 ± 5.45E-03	0.00E+00 ± 0.00E+00	1.49E+00 ± 6.18E-01	4.54E+00 ± 2.12E+00	4.27E-08 ± 3.32E-08	4.03E+00 ± 7.64E-01	0.00E+00 ± 0.00E+00	
f_{19}	4.77E+01 ± 1.97E+01	4.62E+01 ± 3.17E+01	6.29E+01 ± 3.37E+01	4.78E+01 ± 2.05E+01	2.72E+01 ± 1.05E+01	4.63E+01 ± 2.75E-01	6.09E+01 ± 2.59E+01	4.82E+01 ± 3.16E-01	2.38E+03 ± 2.82E+03	1.08E+06 ± 1.50E+06	4.45E+01 ± 1.42E+00	1.56E+02 ± 9.16E+01	4.89E+01 ± 6.64E-02	
f_{20}	4.21E-01 ± 9.83E-02	1.66E+01 ± 5.62E+00	6.55E-01 ± 3.73E-01	6.65E+00 ± 3.79E+00	3.27E+01 ± 7.49E+00	2.65E-04 ± 5.07E-04	5.08E+01 ± 3.08E+00	2.36E-25 ± 7.40E-25	2.34E+02 ± 4.14E+01	5.66E+01 ± 3.72E+01	1.25E+00 ± 3.85E-01	1.98E+02 ± 2.20E+01	0.00E+00 ± 0.00E+00	
f_{21}	6.36E-04 ± 0.00E+00	6.36E-04 ± 2.22E-12	6.36E-04 ± 0.00E+00	6.36E-04 ± 5.69E-12	6.36E-04 ± 0.00E+00	6.36E-04 ± 6.02E-05	6.36E-04 ± 0.00E+00	6.36E-04 ± 6.02E-05	6.36E-04 ± 3.12E+02	6.36E-04 ± 2.64E+02	6.36E-04 ± 2.82E-12	6.36E-04 ± 1.23E-09	0.00E+00 ± 0.00E+00	
f_{22}	3.32E-01 ± 4.27E-02	4.26E-01 ± 1.03E-01	3.76E-01 ± 4.97E-02	4.13E-01 ± 5.97E-02	3.94E-01 ± 6.77E-02	6.23E-01 ± 5.53E-02	6.28E-01 ± 4.79E-02	1.01E+00 ± 1.10E-01	8.46E-01 ± 6.95E-02	1.41E+01 ± 1.01E+01	4.01E-01 ± 5.16E-02	5.66E-01 ± 9.52E-02	9.43E-01 ± 1.61E-01	
f_{23}	4.83E-01 ± 1.59E-01	5.36E-01 ± 2.84E-01	4.80E-01 ± 1.61E-01	5.79E-01 ± 2.30E-01	5.38E-01 ± 1.84E-01	4.39E-01 ± 3.31E-02	4.04E-01 ± 6.39E-02	4.99E-01 ± 2.46E-03	6.97E-01 ± 4.06E-01	1.56E+03 ± 2.99E+03	5.30E-01 ± 1.54E-01	5.29E-01 ± 2.29E-01	5.00E-01 ± 7.20E-04	
f_{24}	7.66E-05 ± 3.83E-05	2.75E+00 ± 1.28E+00	4.68E-06 ± 2.49E-05	5.35E-01 ± 3.56E-01	1.05E+00 ± 4.15E-01	8.91E-12 ± 2.77E-11	5.51E-01 ± 1.94E-02	0.00E+00 ± 0.00E+00	1.75E+01 ± 3.45E+00	1.06E+01 ± 1.06E+01	1.19E-02 ± 4.89E-03	7.38E+00 ± 3.23E+00	0.00E+00 ± 0.00E+00	
f_{25}	4.33E-02 ± 9.31E-03	1.23E-02 ± 2.08E-03	3.32E-02 ± 7.68E-03	1.91E-02 ± 3.12E-03	1.80E-01 ± 5.89E-02	1.16E+00 ± 1.56E-01	2.19E-01 ± 2.54E-02	9.95E-01 ± 2.29E-01	1.48E-02 ± 5.43E-03	4.58E-03 ± 7.93E-03	3.13E+00 ± 2.78E-01	0.00E+00 ± 0.00E+00		
f_{26}	1.17E+00 ± 1.68E-01	1.59E+00 ± 1.52E-01	4.58E+00 ± 1.37E+00	1.34E+00 ± 1.47E-01	1.58E+00 ± 2.43E-01	1.81E+01 ± 5.13E-01	5.05E+00 ± 3.60E-01	0.00E+00 ± 1.00E+00	1.07E+01 ± 2.14E+00	3.18E+00 ± 7.72E-01	6.95E+00 ± 3.09E+00	1.49E+01 ± 8.10E-01	0.00E+00 ± 2.03E+00	
f_{27}	6.53E+00 ± 9.36E-01	6.07E+00 ± 3.72E-01	9.49E+00 ± 1.51E+00	5.40E+00 ± 3.86E-01	9.09E+00 ± 1.33E+00	2.68E+01 ± 1.45E+00	1.87E+01 ± 1.00E+00	0.00E+00 ± 0.00E+00	1.68E+01 ± 2.33E+00	4.10E+01 ± 1.27E+01	3.45E+01 ± 1.87E+00	2.96E+01 ± 7.56E+00	2.20E+01 ± 3.54E-01	
f_{28}	3.01E+01 ± 3.11E+00	1.19E+01 ± 2.33E+00	2.96E+01 ± 1.40E+00	1.26E+01 ± 1.65E+00	1.02E+02 ± 3.72E+01	8.47E+01 ± 5.00E+01	8.43E+01 ± 5.00E+00	1.56E+01 ± 5.42E+01	1.94E+02 ± 3.79E+01	7.67E+01 ± 8.92E+01	2.95E+02 ± 1.55E+01	8.16E+01 ± 2.61E+01	0.00E+00 ± 0.00E+00	
f_{29}	5.37E-03 ± 3.31E-03	2.05E-12 ± 5.49E-12	4.82E-03 ± 2.89E-03	5.54E-10 ± 1.90E-09	9.77E-10 ± 2.27E-09	3.70E-12 ± 1.83E-11	2.09E-01 ± 1.77E-01	1.69E-04 ± 9.25E-04	2.33E+00 ± 9.25E-04	7.92E+00 ± 7.10E+00	2.42E-07 ± 4.20E-07	7.51E-06 ± 1.77E-05	3.31E-132 ± 1.83E-131	
f_{30}	3.94E-16 ± 3.90E-16	5.04E+00 ± 1.95E+00	1.65E-01 ± 3.99E-01	1.15E+00 ± 1.15E+00	1.41E+00 ± 9.85E-01	0.00E+00 ± 0.00E+00	5.17E-01 ± 3.78E-01	0.00E+00 ± 0.00E+00	1.73E+01 ± 1.12E+00	4.14E+03 ± 6.60E+03	2.80E-12 ± 2.76E-12	3.03E+00 ± 1.98E+00	0.00E+00 ± 0.00E+00	
f_{31}	7.99E-11 ± 4.37E-10	7.16E+00 ± 4.21E+00	8.47E-02 ± 1.72E-01	1.71E+00 ± 1.36E+00	4.34E+00 ± 2.63E+00	1.13E-01 ± 3.67E-02	2.18E-01 ± 8.34E-02	3.93E+00 ± 1.75E-01	1.21E+03 ± 7.96E+02	4.89E+03 ± 4.38E+03	7.85E-02 ± 1.75E-01	3.78E+04 ± 3.18E+03	4.52E+00 ± 2.65E-01	
f_{32}	3.36E-02 ± 1.64E-02	4.79E-02 ± 1.76E-02	3.30E-01 ± 2.63E-01	9.13E-03 ± 9.13E-03	3.20E-02 ± 5.20E-01	4.61E-01 ± 7.92E-01	1.01E+00 ± 2.48E-01	1.49E+00 ± 1.84E-05	6.59E-06 ± 1.31E-01	1.05E+00 ± 2.30E+00	5.18E+00 ± 1.42E+00	8.60E-02 ± 8.89E-02	1.83E-07 ± 6.62E-07	

The best results are highlighted in bold.

Table 5 The optimization results obtained by SIDE, 8 DE variants and 4 non-DE-based algorithms at $D = 100$ over independent 30 runs

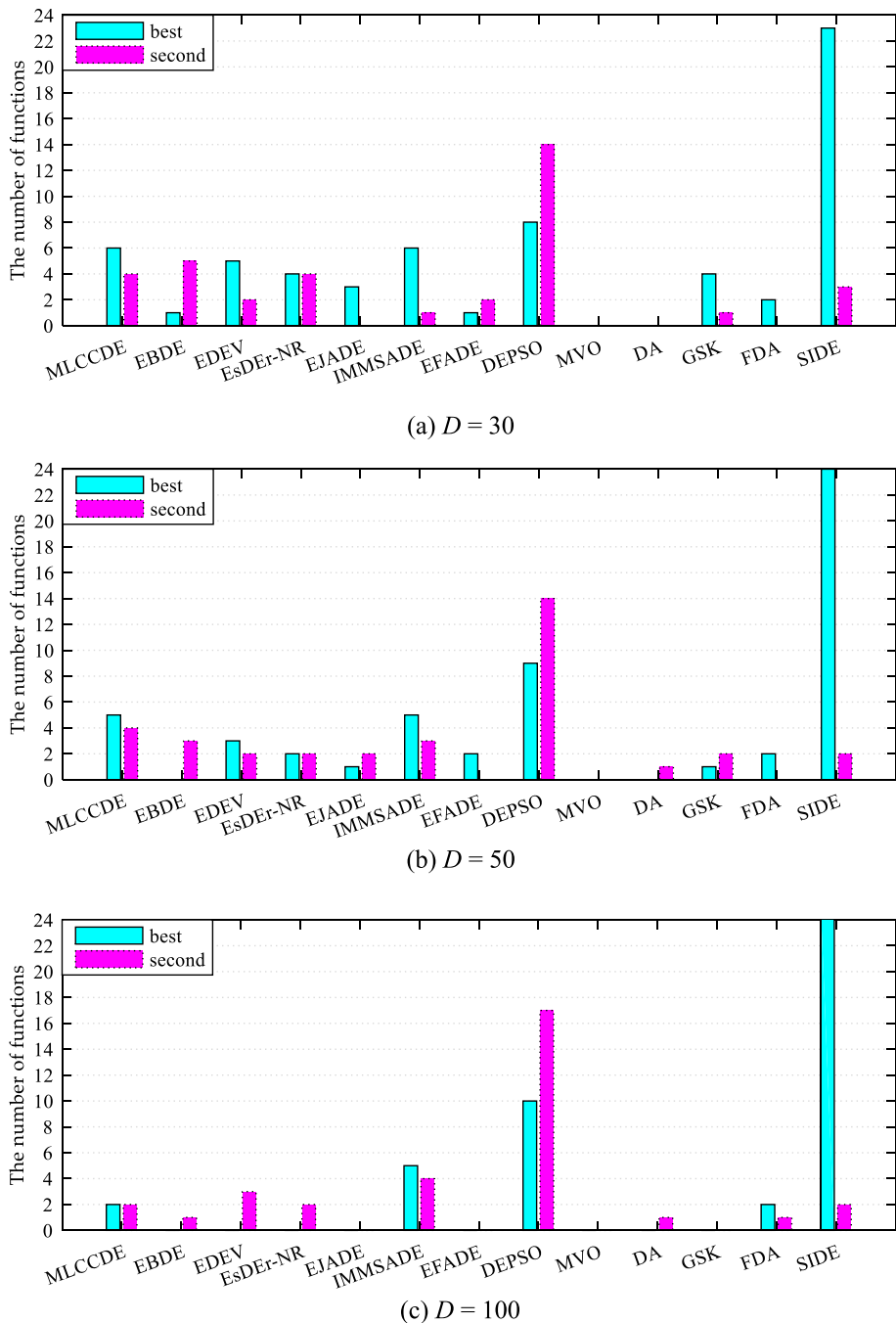
<i>F</i>	Mean \pm STD	MLCDE	EBDE	EDEV	EsDER-NR	EJADE	IMMSADE	EFADE	DEPSO	MVO	DA	GSK	FDA	SIDE
<i>f</i> ₁	1.10E-06 \pm 5.77E-07	1.65E-07 \pm 1.80E-07	8.17E-10 \pm 6.88E-10	5.47E-04 \pm 1.44E-03	1.35E-08 \pm 3.01E-08	4.76E-17 \pm 1.81E-16	2.56E+01 \pm 1.33E+01	8.70E-96 \pm 3.50E-95	1.21E+01 \pm 1.47E+00	3.69E+03 \pm 4.27E+03	2.13E-03 \pm 3.65E-03	9.35E-03 \pm 3.94E-03	0.00E+00 \pm 0.00E+00	
<i>f</i> ₂	3.30E-03 \pm 1.69E-03	6.15E-03 \pm 8.20E-03	2.23E-06 \pm 1.63E-06	1.12E-03 \pm 2.52E+03	8.87E-03 \pm 2.01E-02	5.96E-12 \pm 2.85E-11	4.38E+03 \pm 2.61E+03	2.22E-91 \pm 9.50E-91	4.56E+07 \pm 7.03E+06	4.33E+07 \pm 4.33E+07	1.77E+01 \pm 1.38E+01	3.69E+02 \pm 2.69E+02	0.00E+00 \pm 0.00E+00	
<i>f</i> ₃	1.81E+03 \pm 4.74E+02	2.78E+02 \pm 1.28E+02	3.92E+02 \pm 1.47E+02	6.55E+02 \pm 1.97E+02	1.88E+02 \pm 8.43E+01	1.22E+04 \pm 1.44E+04	9.93E+03 \pm 2.34E+03	5.07E-92 \pm 2.39E-91	1.86E+04 \pm 2.83E+03	7.84E+04 \pm 6.74E+04	5.16E+03 \pm 1.38E+03	1.64E+03 \pm 4.03E+02	8.24E-161 \pm 3.77E-160	
<i>f</i> ₄	5.06E-04 \pm 3.09E-04	1.21E-03 \pm 1.37E-03	2.05E-06 \pm 3.04E-06	7.09E-02 \pm 7.71E-02	4.87E-03 \pm 4.51E-09	1.73E-09 \pm 6.21E-03	2.59E+00 \pm 4.60E-01	7.65E-50 \pm 3.84E-49	5.96E+15 \pm 3.13E+16	2.38E+01 \pm 1.29E+01	2.40E-02 \pm 4.13E-02	2.14E-02 \pm 7.80E-03	9.88E-324 \pm 0.00E+00	
<i>f</i> ₅	5.20E+00 \pm 6.29E-01	1.71E+01 \pm 1.69E+00	1.20E+01 \pm 1.60E+00	1.01E+01 \pm 1.92E+00	1.18E+01 \pm 1.44E+00	5.71E-04 \pm 1.39E-03	5.03E+01 \pm 3.01E+00	1.01E-49 \pm 2.93E-49	3.31E+01 \pm 5.61E+00	2.01E+01 \pm 1.18E+01	7.83E+00 \pm 1.18E+00	2.09E+01 \pm 1.59E+00	2.38E-256 \pm 0.00E+00	
<i>f</i> ₆	3.92E-07 \pm 1.48E-07	1.06E-07 \pm 1.26E-07	2.82E-10 \pm 1.74E-10	4.77E-04 \pm 1.5E-03	1.67E-08 \pm 5.57E-08	3.44E-13 \pm 1.88E-12	9.31E+00 \pm 5.25E+00	5.98E-94 \pm 3.27E-93	5.17E+01 \pm 2.23E+01	1.98E+03 \pm 1.92E+03	4.54E-04 \pm 4.79E-04	1.02E-03 \pm 4.25E-04	0.00E+00 \pm 0.00E+00	
<i>f</i> ₇	4.87E-11 \pm 3.56E-11	1.05E-11 \pm 1.42E-11	9.49E-14 \pm 7.57E-14	1.45E-08 \pm 3.29E-08	9.33E-13 \pm 1.53E-12	4.81E-17 \pm 5.60E-17	6.35E-03 \pm 2.15E-03	0.00E+00 \pm 0.00E+00	6.40E-04 \pm 8.82E-05	1.08E-01 \pm 1.28E-01	1.00E+00 \pm 1.18E-01	3.26E-04 \pm 1.64E-04	0.00E+00 \pm 0.00E+00	
<i>f</i> ₈	1.06E+00 \pm 5.55E-01	1.65E-01 \pm 2.57E-01	1.79E-04 \pm 1.71E-04	7.89E+02 \pm 2.54E+03	1.20E-02 \pm 1.54E-02	2.08E-11 \pm 1.04E-10	2.57E+07 \pm 1.11E+07	7.72E-87 \pm 4.23E-86	1.22E+07 \pm 1.96E+06	4.05E+09 \pm 4.21E+09	6.96E+02 \pm 8.49E+02	4.28E+04 \pm 2.45E+04	0.00E+00 \pm 0.00E+00	
<i>f</i> ₉	8.25E-07 \pm 5.15E-07	1.92E+00 \pm 1.12E+00	1.22E+00 \pm 1.55E+00	5.02E+00 \pm 1.14E+01	1.56E-08 \pm 2.15E-08	8.63E+01 \pm 4.07E+01	2.23E-01 \pm 1.35E-01	3.51E-62 \pm 1.91E-61	1.23E-01 \pm 1.38E-02	1.58E+03 \pm 5.55E+02	2.79E+02 \pm 3.85E+01	3.03E-03 \pm 1.18E-03	1.81E-22 \pm 9.60E-22	
<i>f</i> ₁₀	9.77E-01 \pm 4.31E-01	2.43E-01 \pm 3.35E-01	2.48E-04 \pm 3.05E-04	9.87E-02 \pm 1.28E+03	4.59E-02 \pm 5.18E-02	5.01E-10 \pm 2.54E-09	2.29E+07 \pm 1.33E+07	2.22E-89 \pm 9.80E-89	1.22E+07 \pm 1.87E+06	3.04E-09 \pm 3.50E+09	8.56E+02 \pm 7.38E+02	6.16E+04 \pm 3.27E+04	0.00E+00 \pm 0.00E+00	
<i>f</i> ₁₁	7.00E-01 \pm 9.53E-01	7.80E+01 \pm 3.94E+01	3.20E+00 \pm 5.62E+00	7.61E+01 \pm 2.96E+01	2.93E+01 \pm 9.87E+00	0.00E+00 \pm 0.00E+00	3.20E+01 \pm 1.21E+01	0.00E+00 \pm 0.00E+00	1.07E+02 \pm 2.91E+01	3.80E+03 \pm 4.28E+03	4.13E+00 \pm 2.80E+00	5.35E+01 \pm 2.05E+01	0.00E+00 \pm 0.00E+00	
<i>f</i> ₁₂	4.38E-02 \pm 1.03E-02	9.23E-02 \pm 2.11E-02	8.02E-02 \pm 1.49E-02	5.25E-02 \pm 1.30E-02	1.13E-01 \pm 2.45E-02	1.36E+04 \pm 5.84E-06	6.48E-02 \pm 1.57E-02	1.36E+04 \pm 5.34E-06	1.35E-01 \pm 3.27E-02	1.76E+00 \pm 3.75E+00	1.36E+04 \pm 6.44E-06	3.52E-01 \pm 9.17E-02	1.36E+04 \pm 7.49E-06	
<i>f</i> ₁₃	1.16E-43 \pm 4.19E-43	8.93E-32 \pm 2.90E-31	1.46E-35 \pm 4.09E-35	5.80E-44 \pm 2.93E-43	2.00E-43 \pm 1.04E-42	6.99E-69 \pm 3.83E-68	3.04E-47 \pm 8.82E-47	2.75E-123 \pm 1.06E-122	1.67E-07 \pm 7.77E-08	7.32E-06 \pm 2.01E-05	1.34E-24 \pm 7.19E-24	5.44E-20 \pm 1.77E-19	0.00E+00 \pm 0.00E+00	
<i>f</i> ₁₄	1.46E+02 \pm 1.81E+01	9.58E+01 \pm 9.97E+00	1.97E+02 \pm 1.60E+01	1.02E+02 \pm 9.02E+00	1.34E+02 \pm 6.54E+01	1.36E+04 \pm 2.20E+02	5.61E+02 \pm 1.45E+01	3.32E-02 \pm 1.82E-01	5.86E+02 \pm 6.65E+01	1.99E+02 \pm 1.35E+02	7.86E+02 \pm 2.52E+01	1.64E+02 \pm 4.06E+01	0.00E+00 \pm 0.00E+00	
<i>f</i> ₁₅	2.14E-03 \pm 4.74E-03	1.49E-02 \pm 4.14E-02	7.11E-03 \pm 1.52E-02	1.73E-02 \pm 3.31E-02	2.71E-03 \pm 5.93E-03	3.38E-15 \pm 1.60E-14	1.38E+00 \pm 1.36E-01	0.00E+00 \pm 0.00E+00	1.11E+00 \pm 1.72E-02	2.75E+01 \pm 3.00E+01	8.67E-03 \pm 1.44E-02	1.75E-01 \pm 1.16E-01	0.00E+00 \pm 0.00E+00	
<i>f</i> ₁₆	5.33E-11 \pm 3.01E-11	6.10E-12 \pm 5.52E-12	5.87E-14 \pm 2.84E-14	3.37E-08 \pm 1.36E-07	8.48E-13 \pm 1.38E-12	0.00E+00 \pm 0.00E+00	1.25E-03 \pm 8.02E-04	0.00E+00 \pm 0.00E+00	1.36E-01 \pm 8.34E-05	5.91E-04 \pm 1.69E-01	4.09E-08 \pm 9.56E-08	2.94E-04 \pm 1.70E-04	0.00E+00 \pm 0.00E+00	
<i>f</i> ₁₇	3.46E-07 \pm 2.17E-07	4.95E-08 \pm 7.07E-08	1.90E-10 \pm 7.61E-11	7.59E-05 \pm 1.19E-04	1.99E-09 \pm 1.64E-09	1.46E-15 \pm 7.94E-15	4.52E+00 \pm 3.35E-97	2.80E+00 \pm 3.24E-01	3.54E+02 \pm 3.97E+02	1.91E-04 \pm 3.06E-04	8.03E-03 \pm 3.89E-03	0.00E+00 \pm 0.00E+00		

Table 5 (continued)

<i>F</i>	Mean \pm STD	MLCCDE	EBDE	EDEV	EsDER-NR	EADE	IMMSADE	EFADE	DEPSO	MVO	DA	GSK	FDA	SIDE
f_{18}	2.50E-04 \pm 2.83E-04	3.51E+00 \pm 4.11E-01	1.37E+00 \pm 4.04E-01	2.75E+00 \pm 3.43E-01	1.86E+00 \pm 1.96E-01	9.97E-10 \pm 2.30E-09	3.91E+00 \pm 2.44E-01	0.00E+00 \pm 0.00E+00	4.14E+00 \pm 4.25E+00	7.49E+00 \pm 2.51E+00	3.34E-03 \pm 2.06E-03	7.09E+00 \pm 9.37E-01	0.00E+00 \pm 0.00E+00	
f_{19}	2.53E+02 \pm 5.96E+01	3.51E+02 \pm 1.18E+02	3.33E+02 \pm 1.50E+02	3.42E+02 \pm 1.01E+02	1.58E+02 \pm 4.85E+01	9.69E+01 \pm 2.86E-01	1.08E+03 \pm 4.62E+02	4.04E+04 \pm 8.86E+04	6.95E+07 \pm 1.05E+08	3.37E+03 \pm 1.59E+04	1.00E+03 \pm 8.23E+02	9.89E+01 \pm 2.62E-02	0.00E+00 \pm 0.00E+00	
f_{20}	2.04E+01 \pm 4.03E+00	1.47E+02 \pm 2.89E+01	1.25E+01 \pm 4.45E+00	1.01E+02 \pm 1.52E+01	1.79E+02 \pm 2.22E+01	8.48E-03 \pm 1.44E-02	3.72E+02 \pm 1.57E+01	2.64E-24 \pm 4.11E+01	7.55E+02 \pm 1.13E+02	1.74E+02 \pm 3.72E+00	4.46E+02 \pm 3.14E+01	4.46E+02 \pm 3.14E+01	0.00E+00 \pm 0.00E+00	
f_{21}	1.27E-03 \pm 1.33E-07	1.27E-03 \pm 1.13E-08	1.27E-03 \pm 3.26E-11	1.30E-03 \pm 6.94E-05	1.27E-03 \pm 2.15E-09	1.27E-03 \pm 0.00E+00	3.19E+00 \pm 1.55E+00	1.27E-03 \pm 0.00E+00	6.45E+02 \pm 5.17E+02	2.90E+02 \pm 2.69E+02	1.43E-03 \pm 3.80E-04	5.28E-03 \pm 1.65E-03	1.27E-03 \pm 0.00E+00	
f_{22}	5.08E-01 \pm 5.38E-02	5.88E-01 \pm 8.88E-02	5.22E-01 \pm 6.80E-02	6.57E-01 \pm 6.67E-02	6.58E-01 \pm 9.47E-02	8.54E-01 \pm 6.00E-02	2.31E+00 \pm 9.65E-01	1.14E+00 \pm 4.64E-02	1.00E+00 \pm 9.51E-02	1.83E+01 \pm 1.70E+01	5.69E-01 \pm 7.48E-02	6.19E-01 \pm 8.58E-02	9.45E-01 \pm 1.02E-01	
f_{23}	5.90E-01 \pm 1.91E-01	5.47E-01 \pm 2.47E-01	5.57E-01 \pm 1.93E-01	5.44E-01 \pm 2.46E-01	5.88E-01 \pm 2.34E-01	5.01E-01 \pm 6.34E-02	2.12E+01 \pm 1.42E+01	5.00E-01 \pm 3.29E-10	1.19E+00 \pm 2.05E+00	2.90E+03 \pm 3.82E+03	6.01E-01 \pm 1.87E-01	6.31E-01 \pm 2.15E-01	5.00E-01 \pm 6.30E-07	
f_{24}	2.79E-01 \pm 1.16E-01	2.41E+01 \pm 1.88E+00	1.71E+00 \pm 8.96E-01	1.29E+01 \pm 2.24E+00	1.31E+01 \pm 2.49E+00	1.54E-06 \pm 6.70E-06	1.99E+01 \pm 1.48E+00	0.00E+00 \pm 0.00E+00	7.34E-01 \pm 8.18E+00	2.29E+01 \pm 1.73E+01	1.59E+00 \pm 3.53E-01	2.93E+01 \pm 3.77E+00	0.00E+00 \pm 0.00E+00	
f_{25}	1.23E-01 \pm 1.82E-02	8.55E-02 \pm 7.58E-03	1.87E-01 \pm 5.13E-02	1.08E-01 \pm 1.53E-02	5.53E-01 \pm 1.14E-01	2.00E+00 \pm 1.58E-01	5.87E-01 \pm 4.06E-02	1.84E+00 \pm 5.67E-02	2.06E-01 \pm 4.95E-02	2.73E-04 \pm 3.32E-04	3.93E+00 \pm 3.49E-01	0.00E+00 \pm 0.00E+00	0.00E+00 \pm 0.00E+00	
f_{26}	5.51E+00 \pm 7.18E-01	6.93E+00 \pm 3.98E-01	1.50E+01 \pm 4.21E+00	5.78E+00 \pm 4.78E-01	6.65E+00 \pm 5.89E-01	4.20E+01 \pm 7.16E-01	3.81E+01 \pm 4.67E-01	3.09E+01 \pm 2.45E+00	8.32E+00 \pm 1.89E+00	2.03E+01 \pm 5.99E+00	3.67E+01 \pm 1.73E+00	3.67E+01 \pm 1.27E+00	0.00E+00 \pm 0.00E+00	
f_{27}	2.92E+01 \pm 2.08E+00	2.90E+01 \pm 2.85E+00	3.91E+01 \pm 2.64E+00	2.15E+01 \pm 1.62E+00	3.39E+01 \pm 4.48E+00	6.67E+01 \pm 7.36E+00	9.89E+01 \pm 2.59E+01	0.00E+00 \pm 0.00E+00	5.84E+01 \pm 8.25E+00	1.18E+02 \pm 4.57E+01	8.56E+01 \pm 2.82E+00	1.02E+02 \pm 1.82E+01	0.00E+00 \pm 0.00E+00	
f_{28}	1.15E+02 \pm 1.19E+01	7.61E+01 \pm 4.65E+00	1.40E+02 \pm 8.34E+00	7.72E+01 \pm 4.76E+00	2.49E+02 \pm 1.06E+02	4.75E+02 \pm 9.81E+01	4.22E+02 \pm 2.11E+01	0.00E+00 \pm 0.00E+00	7.63E+02 \pm 7.75E+01	1.71E+02 \pm 1.21E+02	7.36E+02 \pm 2.98E+01	1.55E+02 \pm 4.23E+01	0.00E+00 \pm 0.00E+00	
f_{29}	3.94E-04 \pm 2.10E-04	1.71E-04 \pm 4.74E-04	1.12E-03 \pm 2.90E-03	7.80E-03 \pm 9.03E-03	7.41E-04 \pm 9.45E-04	1.43E-08 \pm 7.61E-08	4.82E+01 \pm 2.03E+00	3.94E-51 \pm 1.42E-50	3.72E+01 \pm 6.44E+00	1.06E+01 \pm 9.71E+00	2.34E-03 \pm 1.86E-03	1.16E-01 \pm 3.72E-01	5.12E-177 \pm 0.00E+00	
f_{30}	3.62E+00 \pm 1.63E+00	1.68E+01 \pm 2.51E+00	7.73E+00 \pm 2.00E+00	2.21E+01 \pm 3.01E+00	1.31E+01 \pm 2.66E+00	4.68E-15 \pm 2.50E-14	1.21E+02 \pm 4.60E+01	0.00E+00 \pm 0.00E+00	7.04E+01 \pm 5.70E+00	1.01E+04 \pm 1.13E+04	9.75E+00 \pm 3.02E+00	2.13E+01 \pm 2.69E+00	0.00E+00 \pm 0.00E+00	
f_{31}	2.08E-01 \pm 2.14E-01	7.73E+01 \pm 3.42E+01	3.87E+00 \pm 3.22E+00	6.38E+01 \pm 2.17E+01	1.27E+02 \pm 5.30E+01	5.58E-05 \pm 2.23E-04	6.69E+02 \pm 1.73E+02	8.48E+00 \pm 1.72E-01	1.47E+04 \pm 4.17E+03	9.11E+03 \pm 1.03E+04	4.18E+00 \pm 1.71E+00	8.91E+04 \pm 5.12E+03	9.10E-01 \pm 2.49E-01	
f_{32}	3.19E-01 \pm 7.31E-02	2.75E-01 \pm 8.29E-02	1.29E+00 \pm 5.95E-01	2.50E-01 \pm 4.73E-02	5.54E-01 \pm 4.14E-01	1.62E-01 \pm 4.45E-01	6.77E+00 \pm 7.01E-01	5.89E-08 \pm 1.02E-07	8.93E-01 \pm 5.18E-01	2.24E+00 \pm 3.25E+00	5.68E+00 \pm 1.02E+00	1.79E-01 \pm 1.43E-01	1.59E-11 \pm 8.25E-11	

The best results are highlighted in bold

Fig. 5 Number of cases on which each algorithm performs the best and the second best in the comparison



ranks for the test problems in which the first algorithm performs worse than the second algorithm. Larger ranks indicate larger performance discrepancy. “Yes” indicates that the performance of SIDE is better than its competitor significantly.

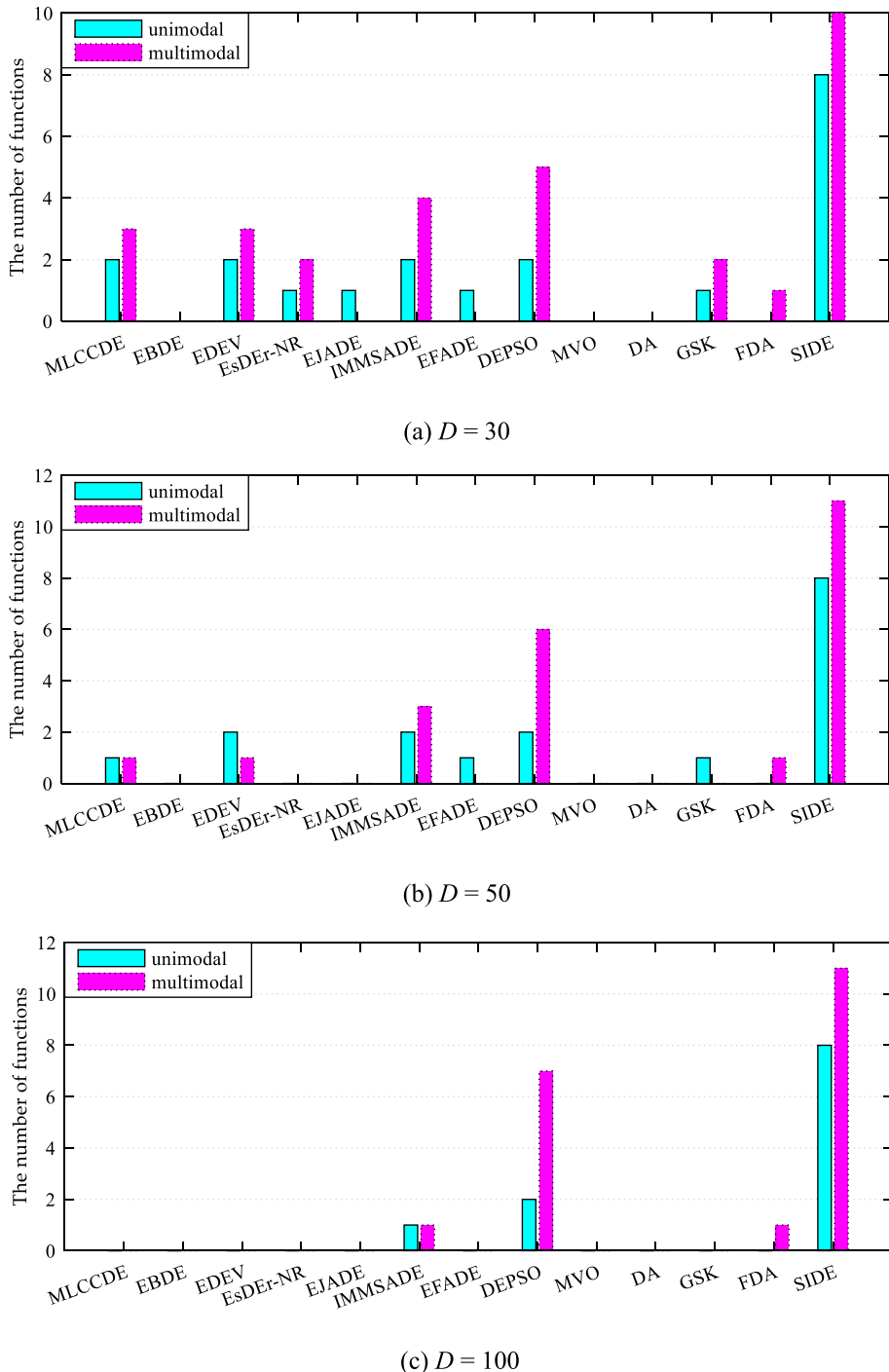
In Fig. 8, SIDE at least outperforms all the compared DE variants in 17, 18, 18 out of 32 functions significantly at $D = 30$, $D = 50$ and $D = 100$, respectively.

Figure 9 shows the average ranks of SIDE and other algorithms according to Friedman test and Kruskal_Wallis

test based on the solution error at $D = 30$, $D = 50$ and $D = 100$, respectively. No matter low-dimensional problems or high-dimensional problems, SIDE gets the first ranking among all algorithms, DEPSO is the second best for 30, 50 and 100 variables.

From a comparative analysis of the results from Tables 9, 10 and 11, it can be seen that SIDE obtains higher R_+ values than R_- in all the cases. It also can be observed that SIDE outperforms all the compared DE variants and non-DE-based algorithms significantly. In

Fig. 6 Number of cases on which each algorithm obtains the global optimum in the comparison



addition, Figs. 7, 8 and Tables 9, 10 and 11 clearly show that the advantage of SIDE is more prominent as the number of dimensions increasing.

Overall, from the above analysis and comparisons, the proposed SIDE is better in term of searching quality, efficiency and robustness. It proves that SIDE greatly keeps the balance between the local optimization speed and the global optimization diversity.

4.4 Performance sensitivity to the population size N_p

The impact of the population size N_p on the performance of SIDE is also investigated. SIDE variants with $N_p = \{50, 75, 125, 150, 175, 200, 225, 250\}$ are compared with the SIDE with $N_p = 100$. Friedman test results are shown in Fig. 10.

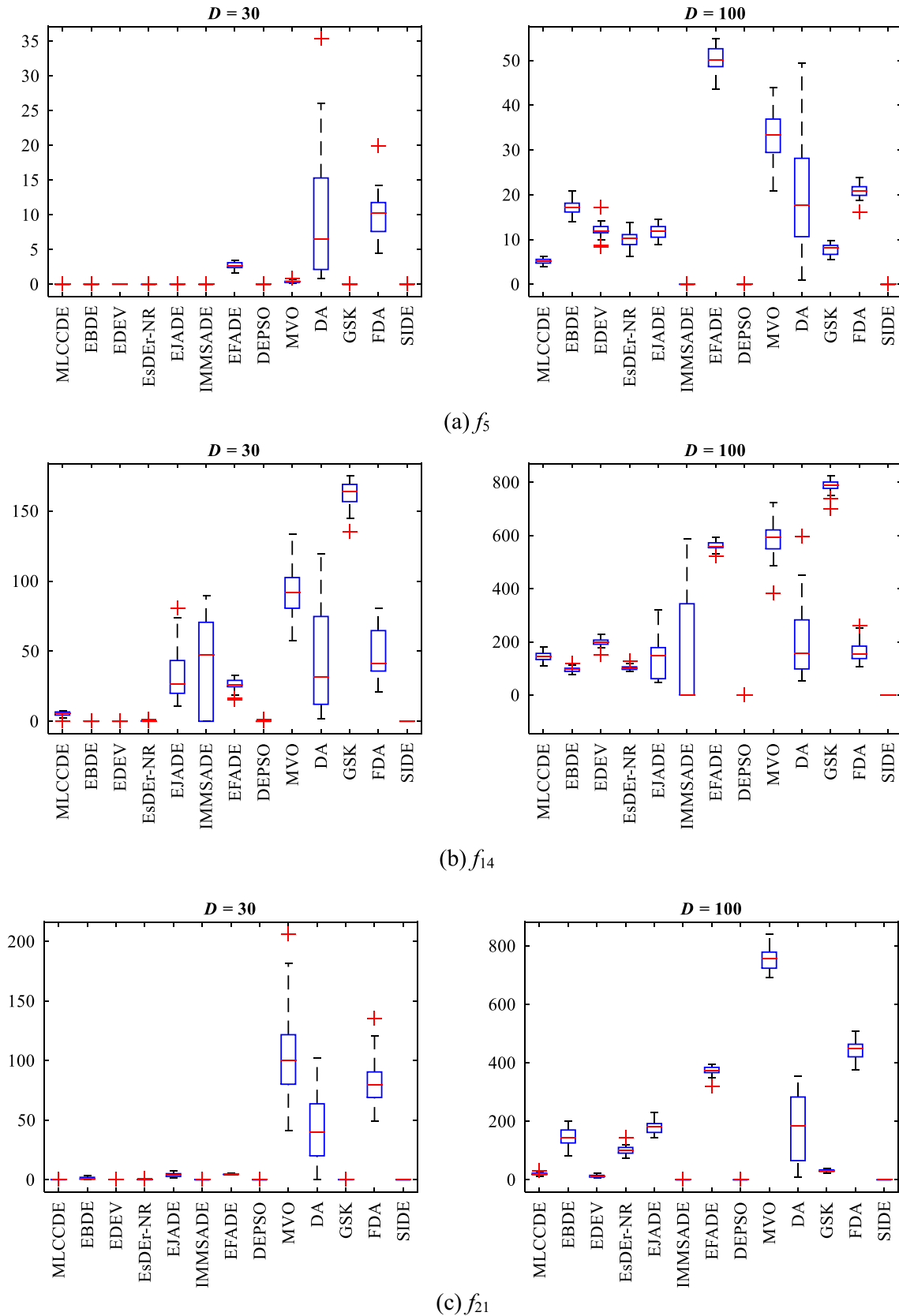


Fig. 7 Box plots of the result of solution error for functions f_5 , f_{14} , f_{21} , f_{26} , f_{28} and f_{32}

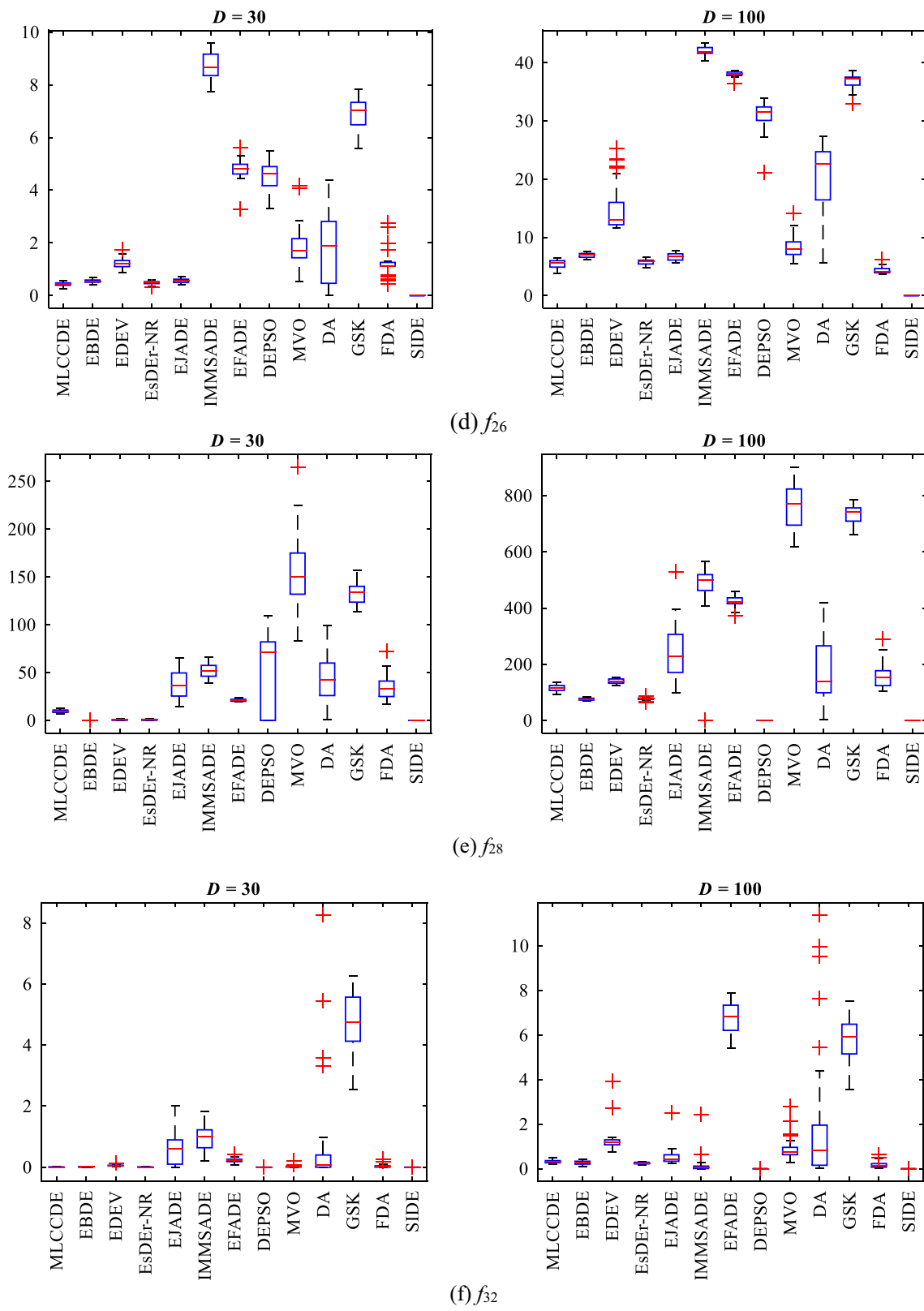
**Fig. 7** continued

Table 6 The MNEG and SR obtained by SIDE, 8 DE variants and 4 non-DE-based algorithms at $D = 30$ over independent 30 runs

<i>F</i>	MNEG(SR%)	MLCCDE	EBDE	EDEV	EsDER-NR	EJADE	IMMSADE	EFADE	DEPSO	MVO	DA	GSK	FDA	SIDE
f_1	410(100)	237(100)	334(100)	226(100)	214(100)	330(100)	841(100)	610(100)	N/A(0)	405(100)	480(100)	15(100)		
f_2	517(100)	339(100)	440(100)	293(100)	292(100)	403(100)	938(100)	636(100)	N/A(0)	490(100)	661(100)	19(100)		
f_3	N/A(0)	816(100)	952(16.7)	708(100)	726(100)	N/A(0)	N/A(0)	631(100)	N/A(0)	N/A(0)	N/A(0)	N/A(0)	22(100)	
f_4	651(100)	387(100)	580(100)	380(100)	382(100)	501(100)	N/A(0)	661(100)	N/A(0)	426(6.7)	626(100)	685(100)	20(100)	
f_5	N/A(0)	N/A(0)	N/A(0)	N/A(0)	643(100)	N/A(0)	892(63.3)	N/A(0)	N/A(0)	N/A(0)	N/A(0)	N/A(0)	25(100)	
f_6	385(100)	223(100)	314(100)	210(100)	198(100)	304(100)	790(100)	604(100)	N/A(0)	435(3.3)	381(100)	487(100)	14(100)	
f_7	278(100)	150(100)	228(100)	152(100)	145(100)	217(100)	821(100)	570(100)	N/A(0)	455(6.7)	N/A(0)	536(100)	10(100)	
f_8	581(100)	354(100)	475(100)	327(100)	318(100)	473(100)	N/A(0)	656(100)	N/A(0)	554(100)	768(100)	21(100)		
f_9	390(100)	864(100)	963(10.0)	861(90.0)	193(100)	N/A(0)	797(100)	655(100)	N/A(0)	N/A(0)	N/A(0)	571(100)	70(100)	
f_{10}	581(100)	384(100)	481(100)	344(100)	333(100)	493(100)	N/A(0)	654(100)	N/A(0)	N/A(0)	554(100)	758(100)	22(100)	
f_{11}	168(100)	118(86.7)	119(100)	91(100)	90(100)	115(100)	405(100)	520(100)	983(6.7)	N/A(0)	192(100)	560(63.3)	6(100)	
f_{12}	N/A(0)	889(3.3)	N/A(0)	N/A(0)	N/A(0)	803(10.0)	N/A(0)	N/A(0)	N/A(0)	511(10.0)	N/A(0)	N/A(0)	N/A(0)	
f_{13}	88(100)	58(100)	72(100)	54(100)	56(100)	57(100)	154(100)	496(100)	956(3.3)	500(13.3)	98(100)	102(100)	4(100)	
f_{14}	N/A(0)	N/A(0)	N/A(0)	N/A(0)	N/A(0)	858(16.7)	N/A(0)	853(96.7)	N/A(0)	N/A(0)	N/A(0)	N/A(0)	34(100)	
f_{15}	423(100)	245(66.7)	357(100)	242(100)	223(96.7)	338(100)	957(100)	613(93.3)	N/A(0)	N/A(0)	422(100)	535(46.7)	126(100)	
f_{16}	280(100)	152(100)	229(100)	153(100)	145(100)	209(100)	629(100)	567(100)	N/A(0)	N/A(0)	290(100)	575(100)	10(100)	
f_{17}	395(100)	224(100)	323(100)	217(100)	204(100)	314(100)	838(100)	603(100)	N/A(0)	N/A(0)	390(100)	478(100)	14(100)	
f_{18}	601(100)	368(96.7)	530(100)	344(100)	337(100)	489(100)	N/A(0)	657(100)	N/A(0)	N/A(0)	584(100)	N/A(0)	20(100)	
f_{19}	N/A(0)	N/A(0)	N/A(0)	N/A(0)	N/A(0)	863(10.0)	N/A(0)							
f_{20}	N/A(0)	N/A(0)	N/A(0)	966(6.7)	N/A(0)	944(3.3)	N/A(0)	763(100)	N/A(0)	462(3.3)	N/A(0)	N/A(0)	39(100)	
f_{24}	873(100)	N/A(0)	873(80.0)	486(80.0)	N/A(0)	625(100)	N/A(0)	674(100)	N/A(0)	457(6.7)	778(60.0)	N/A(0)	22(100)	
f_{25}	N/A(0)	467(43.3)	N/A(0)	2(100)	504(80.0)									
f_{26}	N/A(0)	62(100)												
f_{27}	N/A(0)	46(100)	N/A(0)	412(3.3)	N/A(0)	N/A(0)	N/A(0)							
f_{28}	N/A(0)	934(30.0)	N/A(0)	N/A(0)	N/A(0)	N/A(0)	98(100)							
f_{29}	N/A(0)	385(100)	N/A(0)	530(93.3)	403(100)	555(100)	N/A(0)	654(100)	N/A(0)	441(6.7)	824(96.7)	713(100)	83(100)	
f_{30}	469(100)	274(36.7)	383(100)	257(96.7)	245(93.3)	378(100)	979(50.0)	622(100)	N/A(0)	405(3.3)	455(100)	742(46.7)	16(100)	
f_{31}	490(100)	265(40.0)	440(100)	271(76.7)	244(56.7)	N/A(0)	957(96.7)	N/A(0)	N/A(0)	466(100)	N/A(0)	N/A(0)	N/A(0)	
f_{32}	N/A(0)	898(6.7)	N/A(0)	484(10.0)	N/A(0)	N/A(0)	423(66.7)							

Table 7 The MNEG and SR obtained by SIDE, 8 DE variants and 4 non-DE-based algorithms at $D = 50$ over independent 30 runs

F	MNEG(SR%)	MLCCDE	EBDE	EDEV	EsDE-NR	EJADE	IMMSADE	EFADE	DEPSO	MVO	DA	GSK	FDA	SIDE
f_1	551(100)	433(100)	458(100)	325(100)	321(100)	419(100)	N/A(0)	645(100)	N/A(0)	598(100)	926(90.0)	15(100)		
f_2	710(100)	615(100)	598(100)	530(100)	500(100)	544(100)	N/A(0)	676(100)	N/A(0)	871(90.0)	N/A(0)	20(100)		
f_3	N/A(0)	N/A(0)	N/A(0)	N/A(0)	N/A(0)	N/A(0)	N/A(0)	672(100)	N/A(0)	N/A(0)	N/A(0)	27(100)		
f_4	873(100)	723(100)	746(100)	694(100)	816(96.7)	625(100)	N/A(0)	696(100)	N/A(0)	962(46.7)	N/A(0)	21(100)		
f_5	N/A(0)	N/A(0)	N/A(0)	N/A(0)	N/A(0)	N/A(0)	947(10.0)	N/A(0)	704(100)	N/A(0)	N/A(0)	N/A(0)	26(100)	
f_6	527(100)	411(100)	435(100)	309(100)	297(100)	390(100)	N/A(0)	640(100)	N/A(0)	556(100)	885(100)	15(100)		
f_7	373(100)	273(100)	311(100)	213(100)	194(100)	269(100)	N/A(0)	608(100)	N/A(0)	N/A(0)	N/A(0)	92(93.3)	10(100)	
f_8	800(100)	651(100)	655(100)	480(100)	534(100)	591(100)	N/A(0)	687(100)	N/A(0)	469(10.0)	979(16.7)	N/A(0)	22(100)	
f_9	544(100)	N/A(0)	N/A(0)	N/A(0)	N/A(0)	301(100)	N/A(0)	N/A(0)	695(100)	N/A(0)	N/A(0)	N/A(0)	974(13.3)	146(100)
f_{10}	801(100)	633(100)	668(100)	585(100)	576(100)	612(100)	N/A(0)	689(100)	N/A(0)	997(10.0)	N/A(0)	N/A(0)	23(100)	
f_{11}	228(100)	N/A(0)	173(100)	128(33.3)	131(50.0)	142(100)	656(100)	565(100)	N/A(0)	N/A(0)	240(100)	N/A(0)	6(100)	
f_{12}	101(100)	59(100)	82(100)	59(100)	58(100)	92(100)	179(100)	541(100)	488(100)	440(40.0)	112(100)	106(100)	5(100)	
f_{13}	N/A(0)	N/A(0)	N/A(0)	N/A(0)	N/A(0)	N/A(0)	870(13.3)	N/A(0)	762(93.3)	N/A(0)	N/A(0)	N/A(0)	34(100)	
f_{14}	561(100)	429(36.7)	477(96.7)	333(70.0)	326(76.7)	419(100)	N/A(0)	648(100)	N/A(0)	N/A(0)	632(100)	981(16.7)	72(100)	
f_{15}	380(100)	275(100)	313(100)	211(100)	193(100)	267(100)	977(63.3)	607(100)	N/A(0)	N/A(0)	365(100)	962(46.7)	10(100)	
f_{16}	535(100)	411(100)	441(100)	308(100)	305(100)	383(100)	N/A(0)	645(100)	N/A(0)	N/A(0)	585(100)	906(93.3)	15(100)	
f_{17}	830(100)	737(6.7)	712(100)	515(86.7)	570(100)	619(100)	N/A(0)	691(100)	N/A(0)	N/A(0)	995(3.3)	N/A(0)	21(100)	
f_{18}	N/A(0)	N/A(0)	N/A(0)	N/A(0)	N/A(0)	N/A(0)	N/A(0)	795(100)	N/A(0)	N/A(0)	N/A(0)	N/A(0)	41(100)	
f_{19}	N/A(0)	N/A(0)	939(66.7)	N/A(0)	N/A(0)	789(100)	N/A(0)	679(100)	N/A(0)	464(10.0)	N/A(0)	N/A(0)	23(100)	
f_{20}	N/A(0)	N/A(0)	N/A(0)	N/A(0)	N/A(0)	N/A(0)	N/A(0)	N/A(0)	N/A(0)	583(20.0)	N/A(0)	3(100)	472(100)	
f_{21}	N/A(0)	N/A(0)	N/A(0)	N/A(0)	N/A(0)	N/A(0)	N/A(0)	713(3.3)	N/A(0)	N/A(0)	N/A(0)	N/A(0)	12(100)	
f_{22}	N/A(0)	N/A(0)	N/A(0)	N/A(0)	N/A(0)	N/A(0)	N/A(0)	56(100)	N/A(0)	N/A(0)	N/A(0)	N/A(0)	N/A(0)	
f_{23}	N/A(0)	N/A(0)	N/A(0)	N/A(0)	N/A(0)	N/A(0)	N/A(0)	N/A(0)	N/A(0)	N/A(0)	N/A(0)	N/A(0)	N/A(0)	
f_{24}	N/A(0)	N/A(0)	N/A(0)	N/A(0)	N/A(0)	N/A(0)	N/A(0)	N/A(0)	N/A(0)	N/A(0)	N/A(0)	N/A(0)	N/A(0)	
f_{25}	N/A(0)	N/A(0)	N/A(0)	N/A(0)	N/A(0)	N/A(0)	N/A(0)	N/A(0)	N/A(0)	N/A(0)	N/A(0)	N/A(0)	N/A(0)	
f_{26}	N/A(0)	N/A(0)	N/A(0)	N/A(0)	N/A(0)	N/A(0)	N/A(0)	N/A(0)	N/A(0)	N/A(0)	N/A(0)	N/A(0)	N/A(0)	
f_{27}	N/A(0)	N/A(0)	N/A(0)	N/A(0)	N/A(0)	N/A(0)	N/A(0)	N/A(0)	N/A(0)	N/A(0)	N/A(0)	N/A(0)	N/A(0)	
f_{28}	N/A(0)	N/A(0)	N/A(0)	N/A(0)	N/A(0)	N/A(0)	911(3.3)	N/A(0)	830(86.7)	N/A(0)	N/A(0)	N/A(0)	97(100)	
f_{29}	N/A(0)	648(100)	N/A(0)	651(100)	783(96.7)	586(100)	N/A(0)	688(96.7)	N/A(0)	N/A(0)	983(6.7)	N/A(0)	53(100)	
f_{30}	630(100)	N/A(0)	527(83.3)	N/A(0)	411(13.3)	353(100)	N/A(0)	661(100)	N/A(0)	N/A(0)	735(100)	N/A(0)	17(100)	
f_{31}	666(100)	N/A(0)	552(76.7)	N/A(0)	N/A(0)	N/A(0)	N/A(0)	719(76.7)	N/A(0)	N/A(0)	N/A(0)	N/A(0)	N/A(0)	
f_{32}	N/A(0)	N/A(0)	N/A(0)	N/A(0)	N/A(0)	N/A(0)	791(6.7)	N/A(0)	N/A(0)	N/A(0)	N/A(0)	N/A(0)	173(76.7)	

Table 8 The MNEG and SR obtained by SIDE, 8 DE variants and 4 non-DE-based algorithms at $D = 100$ over independent 30 runs

F	MNEG(SR%)	MLCCDE	EBDE	EDEV	EsDER-NR	EJADE	IMMSADE	EFADE	DEPSO	MVO	DA	GSK	FDA	SIDE
f_1	N/A(0)	N/A(0)	909(100)	N/A(0)	926(73.3)	500(100)	N/A(0)	652(100)	N/A(0)	N/A(0)	N/A(0)	N/A(0)	N/A(0)	17(100)
f_2	N/A(0)	N/A(0)	N/A(0)	N/A(0)	N/A(0)	667(100)	N/A(0)	683(100)	N/A(0)	441(3.3)	N/A(0)	N/A(0)	N/A(0)	21(100)
f_3	N/A(0)	N/A(0)	N/A(0)	N/A(0)	N/A(0)	N/A(0)	N/A(0)	674(100)	N/A(0)	N/A(0)	N/A(0)	N/A(0)	N/A(0)	31(100)
f_4	N/A(0)	N/A(0)	N/A(0)	N/A(0)	N/A(0)	790(93.3)	N/A(0)	699(100)	N/A(0)	N/A(0)	N/A(0)	N/A(0)	N/A(0)	22(100)
f_5	N/A(0)	N/A(0)	N/A(0)	N/A(0)	N/A(0)	N/A(0)	N/A(0)	706(100)	N/A(0)	N/A(0)	N/A(0)	N/A(0)	N/A(0)	27(100)
f_6	N/A(0)	976(3.3)	879(100)	N/A(0)	931(76.7)	501(100)	N/A(0)	653(100)	N/A(0)	N/A(0)	N/A(0)	N/A(0)	N/A(0)	16(100)
f_7	701(100)	703(100)	620(100)	881(76.7)	489(100)	358(100)	N/A(0)	616(100)	N/A(0)	419(3.3)	N/A(0)	N/A(0)	N/A(0)	11(100)
f_8	N/A(0)	N/A(0)	N/A(0)	N/A(0)	N/A(0)	711(100)	N/A(0)	695(100)	N/A(0)	N/A(0)	N/A(0)	N/A(0)	N/A(0)	24(100)
f_9	N/A(0)	N/A(0)	N/A(0)	N/A(0)	N/A(0)	927(56.7)	N/A(0)	N/A(0)	708(100)	N/A(0)	N/A(0)	N/A(0)	N/A(0)	267(100)
f_{10}	N/A(0)	N/A(0)	N/A(0)	N/A(0)	N/A(0)	738(96.7)	N/A(0)	693(100)	N/A(0)	N/A(0)	N/A(0)	N/A(0)	N/A(0)	24(100)
f_{11}	770(50.0)	N/A(0)	809(16.7)	N/A(0)	N/A(0)	183(100)	N/A(0)	573(100)	N/A(0)	N/A(0)	N/A(0)	N/A(0)	N/A(0)	7(100)
f_{13}	114(100)	60(100)	87(100)	65(100)	61(100)	71(100)	209(100)	547(100)	N/A(0)	468(16.7)	134(100)	101(100)	5(100)	
f_{14}	N/A(0)	N/A(0)	N/A(0)	N/A(0)	N/A(0)	834(43.3)	N/A(0)	675(96.7)	N/A(0)	N/A(0)	N/A(0)	N/A(0)	N/A(0)	16(100)
f_{15}	N/A(0)	985(6.7)	903(73.3)	N/A(0)	934(56.7)	528(100)	N/A(0)	654(100)	N/A(0)	421(3.3)	N/A(0)	N/A(0)	N/A(0)	77(100)
f_{16}	708(100)	697(100)	613(100)	867(73.3)	489(100)	324(100)	N/A(0)	616(100)	N/A(0)	N/A(0)	958(16.7)	N/A(0)	N/A(0)	11(100)
f_{17}	N/A(0)	976(33.3)	869(100)	N/A(0)	883(100)	482(100)	N/A(0)	650(100)	N/A(0)	N/A(0)	N/A(0)	N/A(0)	N/A(0)	16(100)
f_{18}	N/A(0)	N/A(0)	N/A(0)	N/A(0)	N/A(0)	776(96.7)	N/A(0)	695(100)	N/A(0)	N/A(0)	N/A(0)	N/A(0)	N/A(0)	22(100)
f_{20}	N/A(0)	N/A(0)	N/A(0)	N/A(0)	N/A(0)	N/A(0)	N/A(0)	799(100)	N/A(0)	N/A(0)	N/A(0)	N/A(0)	N/A(0)	44(100)
f_{24}	N/A(0)	N/A(0)	N/A(0)	N/A(0)	N/A(0)	847(66.7)	N/A(0)	679(100)	N/A(0)	433(6.7)	N/A(0)	N/A(0)	N/A(0)	25(100)
f_{25}	N/A(0)	N/A(0)	N/A(0)	N/A(0)	N/A(0)	N/A(0)	N/A(0)	372(20.0)	N/A(0)	7(100)				484(100)
f_{26}	N/A(0)	N/A(0)	N/A(0)	N/A(0)	N/A(0)	N/A(0)	N/A(0)	N/A(0)	N/A(0)	N/A(0)	N/A(0)	N/A(0)	N/A(0)	73(100)
f_{27}	N/A(0)	N/A(0)	N/A(0)	N/A(0)	N/A(0)	N/A(0)	N/A(0)	109(100)	N/A(0)	N/A(0)	N/A(0)	N/A(0)	N/A(0)	N/A(0)
f_{28}	N/A(0)	N/A(0)	N/A(0)	N/A(0)	N/A(0)	N/A(0)	N/A(0)	728(100)	N/A(0)	N/A(0)	N/A(0)	N/A(0)	N/A(0)	89(100)
f_{29}	N/A(0)	N/A(0)	N/A(0)	N/A(0)	N/A(0)	73(96.7)	N/A(0)	690(100)	N/A(0)	N/A(0)	N/A(0)	N/A(0)	N/A(0)	41(100)
f_{30}	N/A(0)	N/A(0)	N/A(0)	N/A(0)	N/A(0)	554(100)	N/A(0)	665(100)	N/A(0)	N/A(0)	N/A(0)	N/A(0)	N/A(0)	18(100)
f_{32}	N/A(0)	N/A(0)	N/A(0)	N/A(0)	N/A(0)	743(66.7)	N/A(0)	743(66.7)	N/A(0)	N/A(0)	N/A(0)	N/A(0)	N/A(0)	80(100)

Table 9 The results of Wilcoxon rank-sum test at $D = 30$ over 30 independent runs

Comparisons	R +	R-	p value	$\alpha = 0.05$	$\alpha = 0.1$
SIDE versus MLCCDE	217	134	5.25E-03	Yes	Yes
SIDE versus EBDE	358	170	1.06E-04	Yes	Yes
SIDE versus EDEV	214	137	5.96E-03	Yes	Yes
SIDE versus EsDER-NR	255	151	1.67E-03	Yes	Yes
SIDE versus EJADE	340	156	2.09E-04	Yes	Yes
SIDE versus IMMSADE	228	97	3.15E-03	Yes	Yes
SIDE versus EFADE	372	124	1.03E-04	Yes	Yes
SIDE versus DEPSO	216	109	1.79E-02	Yes	Yes
SIDE versus MVO	469	59	2.22E-07	Yes	Yes
SIDE versus DA	502	26	3.35E-09	Yes	Yes
SIDE versus GSK	336	99	3.33E-04	Yes	Yes
SIDE versus FDA	438	90	2.87E-05	Yes	Yes

Table 10 The results of Wilcoxon rank-sum test at $D = 50$ over 30 independent runs

Comparisons	R +	R-	p value	$\alpha = 0.05$	$\alpha = 0.1$
SIDE versus MLCCDE	297	138	1.61E-04	Yes	Yes
SIDE versus EBDE	423	105	7.84E-06	Yes	Yes
SIDE versus EDEV	299	107	2.20E-04	Yes	Yes
SIDE versus EsDER-NR	367	129	1.18E-05	Yes	Yes
SIDE versus EJADE	402	126	1.01E-05	Yes	Yes
SIDE versus IMMSADE	269	82	5.49E-04	Yes	Yes
SIDE versus EFADE	395	101	3.11E-06	Yes	Yes
SIDE versus DEPSO	196	104	1.70E-02	Yes	Yes
SIDE versus MVO	479	49	4.34E-08	Yes	Yes
SIDE versus DA	503	25	2.06E-09	Yes	Yes
SIDE versus GSK	415	81	1.06E-05	Yes	Yes
SIDE versus FDA	449	47	4.61E-06	Yes	Yes

Table 11 The results of Wilcoxon rank-sum test at $D = 100$ over 30 independent runs

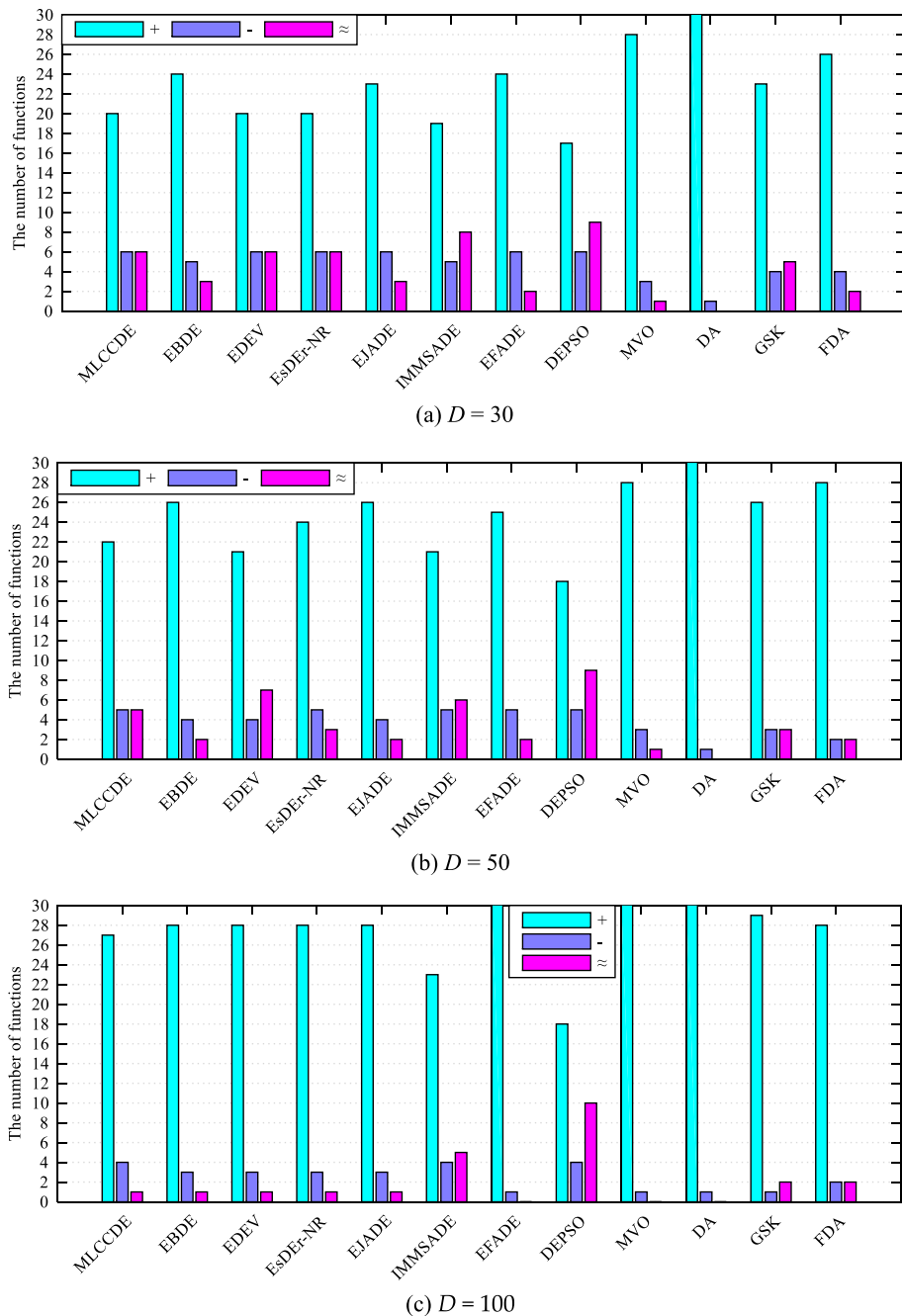
Comparisons	R +	R-	p value	$\alpha = 0.05$	$\alpha = 0.1$
SIDE versus MLCCDE	432	96	1.73E-06	Yes	Yes
SIDE versus EBDE	458	70	8.72E-07	Yes	Yes
SIDE versus EDEV	457	71	1.00E-06	Yes	Yes
SIDE versus EsDER-NR	461	67	2.10E-07	Yes	Yes
SIDE versus EJADE	459	69	8.13E-07	Yes	Yes
SIDE versus IMMSADE	357	78	3.88E-05	Yes	Yes
SIDE versus EFADE	498	30	1.06E-08	Yes	Yes
SIDE versus DEPSO	205	71	3.24E-02	Yes	Yes
SIDE versus MVO	503	25	6.01E-09	Yes	Yes
SIDE versus DA	501	27	1.74E-09	Yes	Yes
SIDE versus GSK	512	16	9.28E-08	Yes	Yes

Although SIDE with $N_p = 200$ is best in Fig. 10, there is no obvious difference in performance in Table 12. In a word, SIDE is not sensitive to the population size N_p .

4.5 Efficiency analysis of proposed algorithmic component

The proposed algorithm represents a combined effect of superior-inferior mutation scheme and the dynamic

Fig. 8 The Wilcoxon's signed-rank test results with a significance level of 0.05 over 30 independent runs

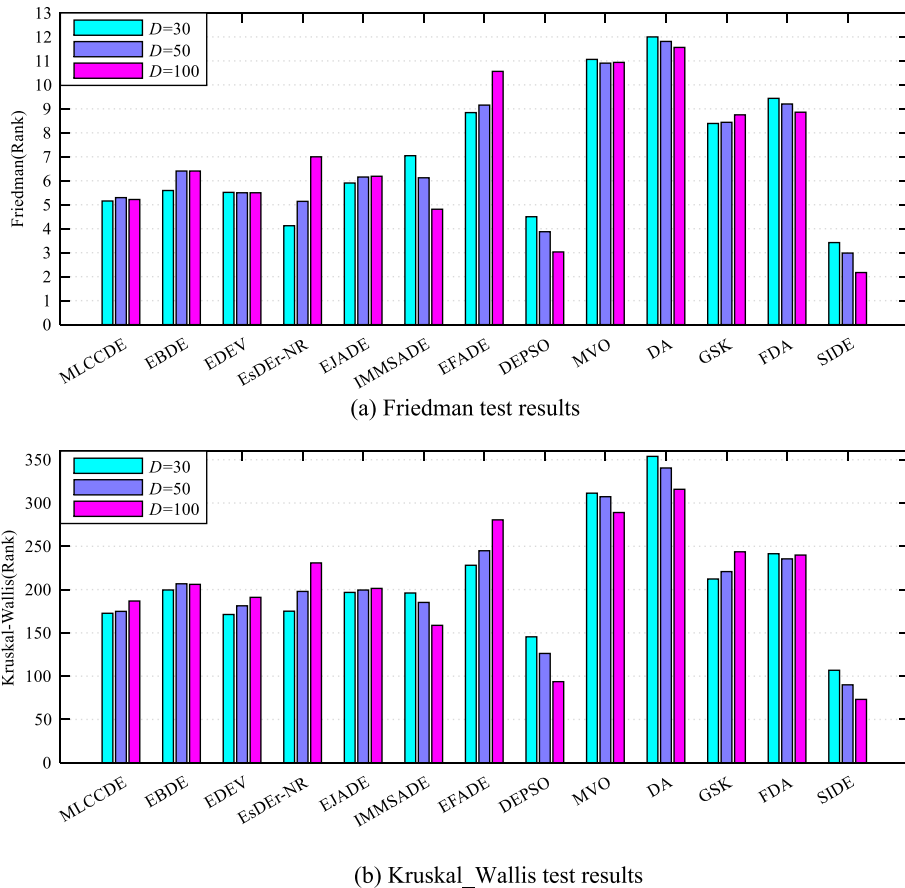


adjustment strategy of exploration factor γ . In order to investigate the efficiency of the proposed algorithmic components, some experiments are conducted. Five SIDE variants with $\gamma = \{0.2, 0.4, 0.6, 0.8, \text{rand}()\}$ have been compared with the proposed SIDE on 32 benchmark functions benchmark at $D = 30$ over 30 independent runs.

Figure 11 shows the rankings of different SIDE variants of applying Friedman test and Kruskal–Wallis test between proposed SIDE and other compared five versions. From Fig. 11, the proposed SIDE is the best, SIDE with $\gamma = \{0.2, \text{rand}()\}$ is the second best, followed by SIDE with $\gamma = \{0.4,$

$0.6, 0.8\}$. From Table 13, there is no obvious performance difference between SIDE and the five SIDE variants. But we can see that proposed SIDE obtains higher R + values than R - values in comparison with its other exploration factor γ . It proves that the superior-inferior mutation scheme has the biggest contribution to SIDE, followed by the dynamic adjustment strategy of γ . It also verifies that superior-inferior mutation scheme and the dynamic adjustment strategy of exploration factor balance the exploration capability and exploitation tendency better.

Fig. 9 Non-parametric test results over 30 independent runs



4.6 Adaptability analysis to high-dimensional problems

Wilcoxon's signed-rank test is performed to evaluate the adaptability to high-dimensional problems for each algorithm between its own 30 variables and 100 variables with the same maximum generation. From the statistical results in Fig. 12, it is easy to observe that:

- (1) The low-dimensional performance of a part of DE variants is significantly better than high-dimensional performance for all the test functions, including EBDE, EsDER-NR, EFADE, MVO and GSK.
- (2) For MLCCDE, EDEV, EJADE and DA, the low-dimensional performance is better than high-dimensional performance in 31 out of 32 functions.
- (3) For SIDE, the low-dimensional performance is better than, worse than and similar to high-dimensional performance in 10, 4 and 18 out of 32 functions, respectively.

We can draw the conclusion that SIDE has the best adaptability to high-dimensional problems respectively.

4.7 Discussions on SIDE

The SIDE algorithm has a considerable ability to maintain its convergence rate, improve its diversity as well as advance its local tendency through a search process. Thus, the proposed SIDE shows competitive performance in terms of quality of solution, efficiency, convergence rate and robustness. The outstanding performance of SIDE stems from three aspects:

1. In the early stage of evolution, superior individual has larger weight, and it is used to guide the population evolving toward the promising solution and improve local exploitation capability.
2. In the later stage of evolution, inferior individual has larger weight, and it can expand the search area to improve population diversity to alleviate the premature convergence.
3. By adjusting the weight of exploration factor dynamically, there is a better balance between the local exploitation and global exploration to improve the global optimization capability of DE.

Fig. 10 The Friedman test results at $D = 30$ over 30 independent runs

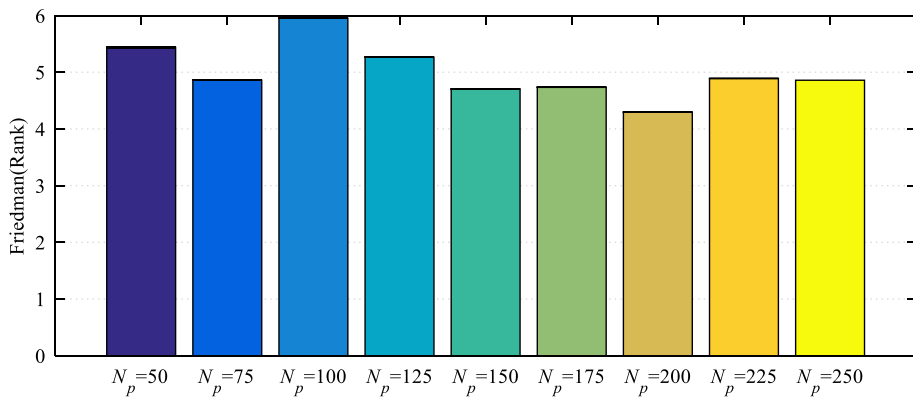


Table 12 The results of Wilcoxon's rank-sum test over 30 independent runs

Comparison	R +	R -	p value	$\alpha = 0.05$	$\alpha = 0.1$
SIDE with $N_p = 200$ versus SIDE with $N_p = 50$	51	4	9.62E-01	No	No
SIDE with $N_p = 200$ versus SIDE with $N_p = 75$	39	6	9.87E-01	No	No
SIDE with $N_p = 200$ versus SIDE with $N_p = 100$	78	13	4.78E-01	No	No
SIDE with $N_p = 200$ versus SIDE with $N_p = 125$	37	8	9.87E-01	No	No
SIDE with $N_p = 200$ versus SIDE with $N_p = 150$	40	5	9.75E-01	No	No
SIDE with $N_p = 200$ versus SIDE with $N_p = 175$	36	9	9.62E-01	No	No
SIDE with $N_p = 200$ versus SIDE with $N_p = 225$	41	4	9.49E-01	No	No
SIDE with $N_p = 200$ versus SIDE with $N_p = 250$	35	10	9.62E-01	No	No

"No" indicates that the performance of SIDE with $N_p = 200$ is similar to its competitor

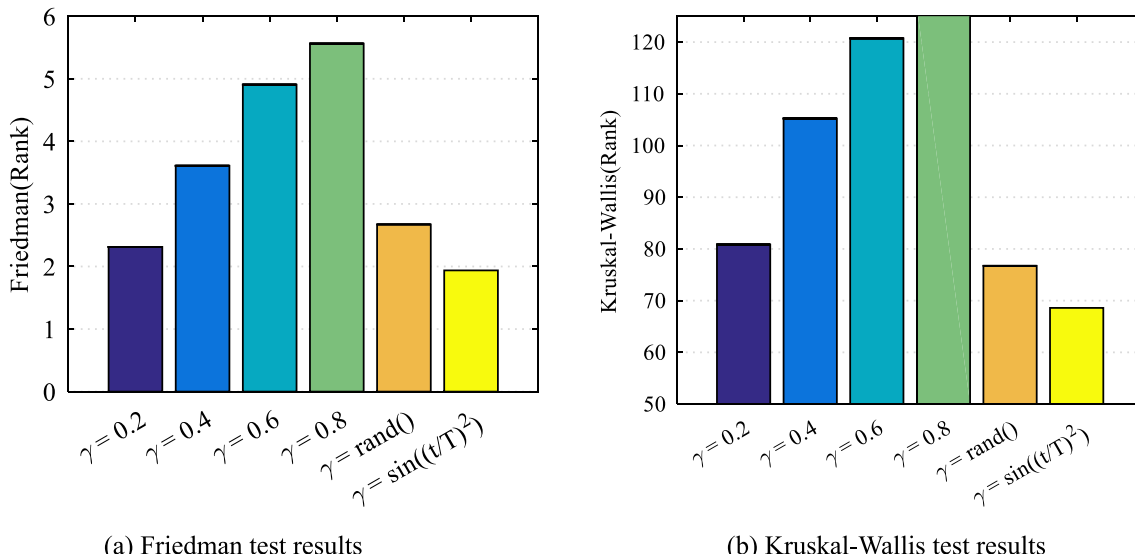


Fig. 11 The Friedman test and Kruskal–Wallis test results at $D = 30$ over 30 independent runs

5 Conclusions

In order to further balance the convergence and diversity, a superior-inferior mutation scheme is proposed in the paper. Furthermore, novel dynamic weight adjustment strategy of superior individual and inferior individual are introduced according to the evolutionary property. Based on the above

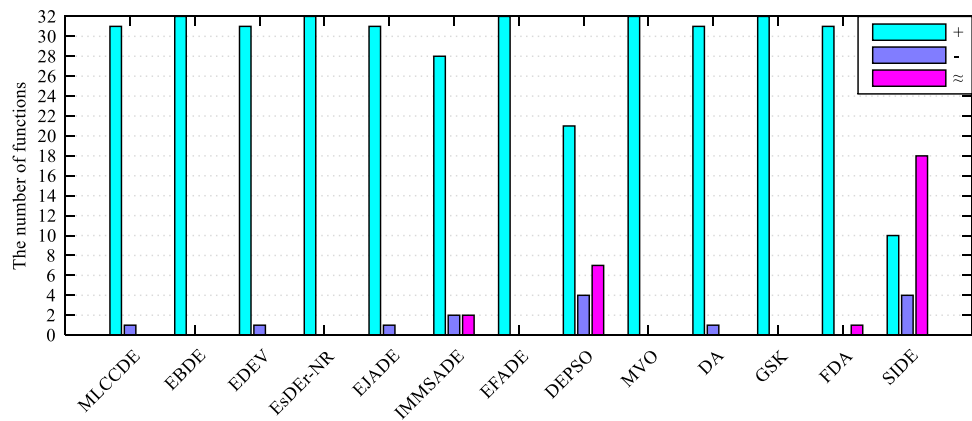
experiments, the effectiveness and efficiency of proposed algorithmic components are verified. Extensive numerical experiments and comparisons comparing with 8 advanced DE algorithms and 4 non-DE-based algorithms have demonstrated the high effectiveness of proposed SIDE. The advantages of proposed SIDE are more obvious as the number of dimensions increase.

Table 13 The results of Wilcoxon's rank-sum test between SIDE with $\gamma = \sin((t/T)^2)$ and SIDE with $\gamma = \{0.2, 0.4, 0.6, 0.8, \text{rand}()\}$ over 30 independent runs

Comparison	R +	R -	p value	$\alpha = 0.05$	$\alpha = 0.1$
SIDE with $\gamma = \sin((t/T)^2)$ versus with $\gamma = 0.2$	143	28	4.350921e-01	No	No
SIDE with $\gamma = \sin((t/T)^2)$ versus with $\gamma = 0.4$	335	16	5.714192e-03	Yes	No
SIDE with $\gamma = \sin((t/T)^2)$ versus with $\gamma = 0.6$	462	34	9.734839e-05	Yes	No
SIDE with $\gamma = \sin((t/T)^2)$ versus with $\gamma = 0.8$	510	18	3.156868e-05	Yes	No
SIDE with $\gamma = \sin((t/T)^2)$ versus with $\gamma = \text{rand}()$	101	19	5.407827e-01	No	No

"No" indicates that the performance of SIDE with $\gamma = \sin((t/T)^2)$ is similar to its competitor. "Yes" indicates that the performance of SIDE with $\gamma = \sin((t/T)^2)$ is better than its competitor significantly

Fig. 12 The Wilcoxon's signed-rank test results with a significance level of 0.05 over 30 independent runs. Signs “+”, “-” and “≈” indicate the number of functions that the performance of algorithm for low dimensional problems is better than, worse than and similar to the performance for high dimensional problems, respectively



As future work, novel control parameters optimization strategies will be studied to solve more complex engineering optimization problems. In addition, SIDE will be applied to various optimization fields, such as carrier aircraft landing sequencing, etc.

Acknowledgements The authors would like to thank anonymous reviewers of Soft Computing for their careful and helpful comments.

Funding This work is supported by Intelligent Policing Key Laboratory of Sichuan Province (Grant no. ZNJW2022KFMS004) and the Science and Technology Program of Sichuan Province, China (Grand No. 2023YFG0264).

Data availability The manuscript has no associated data. The data used is included in the manuscript.

Declarations

Conflict of interest The authors declare that they have no conflict of interest.

Ethical approval This article does not contain any studies with human participants or animals performed by any of the authors.

References

- Ahmed OH, Lu J, Xu Q, Ahmed AM, Rahmani AM, Hosseinzadeh M (2021) Using differential evolution and Moth-Flame optimization for scientific workflow scheduling in fog computing. *Appl Soft Comput* 112:107744
- Ali WM, Suganthan PN (2018) Real-parameter unconstrained optimization based on enhanced fitness-adaptive differential evolution algorithm with novel mutation. *Soft Comput* 22:3215–3235
- Ali WM, Anas AH, Ali KM (2020) Gaining-sharing knowledge based algorithm for solving optimization problems: a novel nature-inspired algorithm. *Int J Mach Learn Cybern* 1:1501–1529
- Ali WM, Ali KM (2017) Adaptive guided differential evolution algorithm with novel mutation for numerical optimization. *Int J Mach Learn Cybern* 1–23
- Altay EV, Alatas B (2021) Differential evolution and sine cosine algorithm based novel hybrid multi-objective approaches for numerical association rule mining. *Inf Sci* 554:198–221
- Arce F, Zamora E, Sossa H, Barrón R (2018) Differential evolution training algorithm for dendrite morphological neural networks. *Appl Soft Comput* 68:303–313
- Awad NH, Ali MZ, Suganthan PN (2018) Ensemble of parameters in a sinusoidal differential evolution with niching-based population reduction. *Swarm Evol Comput* 39:141–156
- Awad NH, Ali MZ, Suganthan PN, Reynolds RG (2016) An ensemble sinusoidal parameter adaptation incorporated with L-SHADE for solving CEC2014 benchmark problems. In: proceedings of the IEEE congress on evolutionary computation, pp 2958–2965
- Awad NH, Ali MZ, Suganthan PN, Liang JJ, Qu BY (2017) Problem definitions and evaluation criteria for the CEC 2017 special session and competition on single objective real-parameter numerical optimization
- Cai YQ, Wang JH (2015) Differential evolution with hybrid linkage crossover. *Inf Sci* 320:244–287
- Cai YQ, Sun G, Wang T et al (2017) Neighborhood-adaptive differential evolution for global numerical optimization. *Appl Soft Comput* 59:659–706
- Chakraborty S, Sharma S, Saha AK, Chakraborty S (2021) SHADE-WOA: a metaheuristic algorithm for global optimization. *Appl Soft Comput* 113:107866

- Chen X (2020) Novel dual-population adaptive differential evolution algorithm for large-scale multi-fuel economic dispatch with valve-point effects. *Energy* 203:117874
- Cui LZ, Li GH, Zhu ZX et al (2018) Adaptive multiple-elites-guided composite differential evolution algorithm with a shift mechanism. *Inf Sci* 422:122–142
- Derrac J, Garcia S, Molina D et al (2011) A practical tutorial on the use of nonparametric statistical tests as a methodology for comparing evolutionary and swarm intelligence algorithms. *Swarm Evolut Comput* 1:3–18
- Ghosh A, Das S, Mullick SS et al (2017) A switched parameter differential evolution with optional blending crossover for scalable numerical optimization. *Appl Soft Comput* 57:329–352
- Gong WY, Cai ZH (2013) Differential evolution with ranking-based mutation operators. *IEEE Trans Cybern* 43:2066–2081
- Gong WY, Cai ZH, Wang Y (2014) Repairing the crossover rate in adaptive differential evolution. *Appl Soft Comput* 15:149–168
- Guo SM, Yang CC (2015) Enhancing differential evolution utilizing eigenvector-based crossover operator. *IEEE Trans Evolut Comput* 19:31–49
- He XY, Zhou YR (2018) Enhancing the performance of differential evolution with covariance matrix self-adaptation. *Appl Soft Comput* 64:227–243
- Houssein EH, Mahdy MA, Blondin MJ, Shebl D, Mohamed WM (2021) Hybrid slime mould algorithm with adaptive guided differential evolution algorithm for combinatorial and global optimization problems. *Expert Syst Appl* 174:114689
- Karami H, Anaraki MV, Farzin S, Mirjalili S (2021) Flow direction algorithm (FDA): a novel optimization approach for solving optimization problems. *Comput Ind Eng* 156:107224
- Le DL, Vo ND, Nguyen TH, et al. (2013) A hybrid differential evolution and harmony search for non-convex economic dispatch problems. In: IEEE conference on power engineering and optimization, pp 238–243
- Li X, Yin M (2012) Hybrid differential evolution with artificial bee colony and its application for design of a reconfigurable antenna array with discrete phase shifters. *Iet Microw Antenna Propag* 6:1573–1582
- Li Y, Wang S, Yang Bo (2020a) An improved differential evolution algorithm with dual mutation strategies collaboration. *Expert Syst Appl* 153:113451
- Li S, Qiong Gu, Gong W, Ning B (2020b) An enhanced adaptive differential evolution algorithm for parameter extraction of photovoltaic models. *Energy Convers Manage* 205:112443
- Liang JJ, Qu BY, Suganthan PN, Hernández-Díaz AG (2013) Problem definitions and evaluation criteria for the CEC 2013 special session on real-parameter optimization
- Liu D, Zhongbo H, Qinghua S, Liu M (2021) A niching differential evolution algorithm for the large-scale combined heat and power economic dispatch problem. *Appl Soft Comput* 113:108017
- Mallipeddi R, Suganthan PN, Pan QK, Tasgetiren MF (2011) Differential evolution algorithm with ensemble of parameters and mutation strategies. *Appl Soft Comput* 11:1679–1696
- Mirjalili S (2016) Dragonfly algorithm: a new meta-heuristic optimization technique for solving single-objective, discrete, and multi-objective problems. *Neural Comput Appl* 27:1053–1073
- Mirjalili S, Mirjalili SM, Hatamlou A (2016) Multi-Verse Optimizer: a nature-inspired algorithm for global optimization. *Neural Comput Appl* 27:495–513
- Mohamed Ali W, Hadi AA, Jambi KM (2019) Novel mutation strategy for enhancing SHADE and LSHADE algorithms for global numerical optimization. *Swarm Evol Comput* 50:100455
- Myszkowski PB, Olech ŁP, Laszczyk M, Skowroński ME (2018) Hybrid differential evolution and greedy algorithm (DEGR) for solving multi-skill resource-constrained project scheduling problem. *Appl Soft Comput* 62:1–14
- Nadimi-Shahraki MH, Taghian S, Mirjalili S, Faris H (2020) MTDE: an effective multi-trial vector-based differential evolution algorithm and its applications for engineering design problems. *Appl Soft Comput* 97:106761
- Nasimul N, Danushka B, Hitoshi I (2011) An adaptive differential evolution algorithm. In: IEEE congress on evolutionary computation, pp 229–236
- Nenavath H, Jatot RK (2018) Hybridizing sine cosine algorithm with differential evolution for global optimization and object tracking. *Appl Soft Comput* 62:1019–1043
- Nguyen-Van S, Nguyen KT, Luong VH, Lee S, Lieu QX (2021) A novel hybrid differential evolution and symbiotic organisms search algorithm for size and shape optimization of truss structures under multiple frequency constraints. *Expert Syst Appl* 184:115534
- Peng H, Han Y, Deng C, Wang J, Zhijian Wu (2021) Multi-strategy co-evolutionary differential evolution for mixed-variable optimization. *Knowl Based Syst* 229:107366
- Ponsich A, Coello CAC (2013) A hybrid differential evolution-Tabu search algorithm for the solution of job-shop scheduling problems. *Appl Soft Comput* 13:462–474
- Qin AK, Huang VL, Suganthan PN (2009) Differential evolution algorithm with strategy adaption for global numerical optimization. *IEEE Trans Evolut Comput* 13:398–417
- Qiu X, Tan KC, Xu JX (2017) Multiple exponential recombination for differential evolution. *IEEE Trans Cybern* 47:995–1005
- Ryoji T, Alex F (2013) Success-history based parameter adaptation for differential evolution. In: IEEE congress on evolutionary computation, pp 71–78
- Storn R, Price K (1995) Differential evolution: a simple and efficient adaptive scheme for global optimization over continuous spaces
- Suganthan PN, Hansen N, Liang J, Deb K (2005) Problem definitions and evaluation criteria for the CEC 2005 special session on real-parameter optimization
- Sun G, Cai YQ, Wang T et al (2018) Differential evolution with individual-dependent topology adaptation. *Inf Sci* 450:1–38
- Tan Z, Li K (2021) Differential evolution with mixed mutation strategy based on deep reinforcement learning. *Appl Soft Comput* 111:107678
- Tang RL (2017) Decentralizing and coevolving differential evolution for large-scale global optimization problems. *Appl Intell* 47:1208–1223
- Tian L, Li Z, Yan X (2020) High-performance differential evolution algorithm guided by information from individuals with potential. *Appl Soft Comput* 95:106531
- Vaisakh K, Praveena P, Sujata KN (2013) Differential evolution and bacterial foraging optimization based dynamic economic dispatch with non-smooth fuel cost functions. In: international conference on swarm, evolutionary, and memetic computing, pp 583–594
- Wang Y, Cai Z, Zhang Q (2011) Differential evolution with composite trial vector generation strategies and control parameters. *IEEE Trans Evolut Comput* 15:55–66
- Wang SH, Li YZ, Yang HY (2017) Self-adaptive differential evolution algorithm with improved mutation mode. *Appl Intell* 47:644–658
- Wang SH, Li YZ, Yang HY (2019) Self-adaptive mutation differential evolution algorithm based on particle swarm optimization. *Appl Soft Comput* 81:105496
- Wei ZK, Xie XL, Bao TT, Yu Y (2019) A random perturbation modified differential evolution algorithm for unconstrained optimization problems. *Soft Comput* 23(15):6307–6321

- Wu GH, Mallipeddi R, Suganthan PN et al (2016) Differential evolution with multi-population based ensemble of mutation strategies. *Inf Sci* 329:329–345
- Wu GH, Shen X, Li H et al (2018) Ensemble of differential evolution variants. *Inf Sci* 423:172–186
- Xu YL, Fang JA, Zhu W et al (2015) Differential evolution using a superior-inferior crossover scheme. *Comput Optim Appl* 61:243–274
- Yildizdan G, Baykan ÖK (2020) A novel modified bat algorithm hybridizing by differential evolution algorithm. *Expert Syst Appl* 141:112949
- Yu X, Li C, Yen GG (2021) A knee-guided differential evolution algorithm for unmanned aerial vehicle path planning in disaster management. *Appl Soft Comput* 98:106857
- Zhang SX, Zheng LM, Tang KS, Zheng SY, Chan WS (2019) Multi-layer competitive-cooperative framework for performance enhancement of differential evolution. *Inf Sci* 482:86–104
- Zhang SX, Chan WS, Peng ZK, Zheng SY, Tang KS (2020) Selective-candidate framework with similarity selection rule for evolutionary optimization. *Swarm Evol Comput* 56:100696
- Zhang SX, Chan WS, Tang KS, Zheng SY (2021a) Adaptive strategy in differential evolution via explicit exploitation and exploration controls. *Appl Soft Comput* 107:107494
- Zhang X, Jin L, Cui C, Sun J (2021b) A self-adaptive multi-objective dynamic differential evolution algorithm and its application in chemical engineering. *Appl Soft Comput* 106:107317
- Zheng LM, Zhang SX, Tang KS, Zheng SY (2017) Differential evolution powered by collective information. *Inf Sci* 399:13–29

Publisher's Note Springer Nature remains neutral with regard to jurisdictional claims in published maps and institutional affiliations.

Springer Nature or its licensor (e.g. a society or other partner) holds exclusive rights to this article under a publishing agreement with the author(s) or other rightsholder(s); author self-archiving of the accepted manuscript version of this article is solely governed by the terms of such publishing agreement and applicable law.